

Review

Photocatalytic Decomposition of Acetaldehyde on Different TiO₂-Based Materials: A Review

Beata Tryba *, Piotr Rychtowski, Agata Markowska-Szczupak and Jacek Przepiórski

Department of Chemical Technology and Engineering, West Pomeranian University of Technology, Szczecin, ul. Pulaskiego 10, 70-322 Szczecin, Poland; rp43903@zut.edu.pl (P.R.); agata.markowska@zut.edu.pl (A.M.-S.); jacek.przepiorski@zut.edu.pl (J.P.)

* Correspondence: beata.tryba@zut.edu.pl; Tel.: +48-609573930

Received: 6 November 2020; Accepted: 12 December 2020; Published: 15 December 2020



Abstract: Purification of air from the organic contaminants by the photocatalytic process has been confirmed to be very perspective. Although many various photocatalysts have been prepared and studied so far, TiO₂ is still the most commonly used, because of its advantageous properties such as non-toxicity, relatively low cost and high stability. Surface modifications of TiO₂ were extensively proceeded in order to increase photocatalytic activity of the photocatalyst under both UV and visible light activations. The intention of this review paper was to summarize the scientific achievements devoted to developing of TiO₂-based materials considered as photocatalysts for the photocatalytic degradation of acetaldehyde in air. Influence of the preparation and modification methods on the parameters of the resultant photocatalyst is reviewed and discussed in this work. Affinity of the photocatalyst surfaces towards adsorption of acetaldehyde will be described by taking into account its physicochemical parameters. Impact of the contact time of a pollutant with the photocatalyst surface is analyzed and discussed with respect to both the degradation rate and mineralization degree of the contaminant. Influence of the photocatalyst properties on the mechanism and yield of the photocatalytic reactions is discussed. New data related to the acetaldehyde decomposition on commercial TiO₂ were added, which indicated the different mechanisms occurring on the anatase and rutile structures. Finally, possible applications of the materials revealing photocatalytic activity are presented with a special attention paid to the photocatalytic purification of air from Volatile Organic Compounds (VOCs).

Keywords: photocatalysis; acetaldehyde removal; titania dioxide; FTIR

1. Introduction

The assurance of good-quality conditions in the indoor air has started to be a subject of many discussions and a wide area of the research studies. Recently, people spend much time inside rooms, and they are exposed to some of the pollutants (mostly VOCs—Volatile Organic Compounds), which are generated by the biological activity of human/animal beings but are also released from the building materials. These VOCs are suspected to induce so-called Sick Building Syndrome, which causes numerous health problems, such as headache and eye, nose, and throat irritation [1]. The effect of the polluted indoor air on human health is schematically illustrated in Figure 1.

According to the classification provided by companies to ECHA (European Chemicals Agency) in REACH (Registration, Evaluation and Authorization of Chemicals) registrations, acetaldehyde was identified as a substance which is suspected of causing cancer. Formaldehyde was also classified as a cancerogenic substance and its concentration in wooden products is regulated under the TSCA (Toxic Substances Control Act) program in the United States. According to the European Standard, for woodgrain boards in E1 class used for indoor application, the maximum concentration of

formaldehyde should not be higher than 0.1 ppm (0.125 mg/m³). The concentration of VOCs in the indoor air is not high, however it can be dangerous for human health. Therefore, some of air cleaning processes can be utilized to solve this problem [2,3]. Recently, one of the most explored methods of VOCs degradation is photocatalysis, with application of TiO₂ as the photocatalyst [4,5]. TiO₂ is commonly used as an additive to the different building materials or can just simply be used as a coating for many building constructions [6,7]. A lot of patents on TiO₂ preparation and utilization have been developed and the interest of the business companies in this matter has greatly increased [8]. In 2010, the technical committee in Europe elaborated some ISO (International Organization for Standardization) standards for testing methods of photocatalytic activity of semiconductor photocatalysts [9]. In total, eight tests under ISO standards were proposed, for performance in water, air and for self-cleaning surfaces. Acetaldehyde, together with toluene and NO_x-group gases, was proposed as a model compound for evaluation of the photocatalytic activity of tested materials in air. Therefore, acetaldehyde is commonly used in the research studies for determination of the photocatalytic activity of different semiconductor materials.

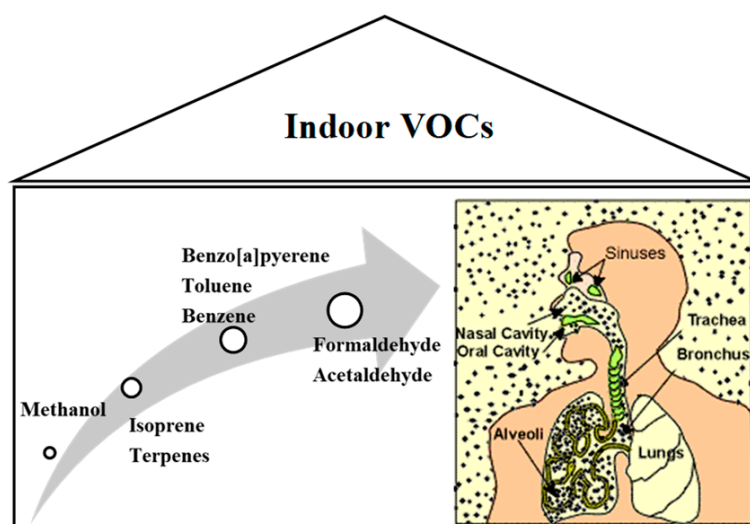


Figure 1. Impact of indoor Volatile Organic Compounds (VOCs) on human health.

Application of TiO₂ for decomposition of low-concentration VOCs was firstly proposed by the group of Fujishima [10]. They reported that even an ordinary room light may be sufficient to help to purify the air or to keep the walls clean in the indoor environment, because the amounts of pollutants are typically small. They assumed that the intensity of UV light of 1 $\mu\text{W}/\text{cm}^2$ was sufficient to decompose a hydrocarbon layer of approximately 1 μm thick every hour [10]. Moreover, they demonstrated that the maximum quantum yield (QY) for decomposition of 2-propanol on TiO₂—28%, was achieved for the lowest light intensity and for the highest concentration of 2-propanol (1000 ppmv) [10]. The explanation of these results was that adsorbed organic molecules helped to inhibit recombination. It was also found that the measured QY values, that could be attributed to a reaction involving hydroxyl radicals, were several orders of magnitude smaller than those that could be attributed to reactions involving holes [10]. However, the maximum QY depends on the intrinsic quality of TiO₂ and its ability of rapid bulk recombination. Therefore, suppressing of electron/hole pairs recombination in TiO₂ can significantly improve its photocatalytic activity. In the proposed mechanism of acetaldehyde decomposition, the radical-initiated chain reactions with oxygen consumption were illustrated [10]. The schematic diagram of processes occurring during photocatalytic oxidation of acetaldehyde on an illuminated TiO₂ particle is illustrated in Figure 2 [10].

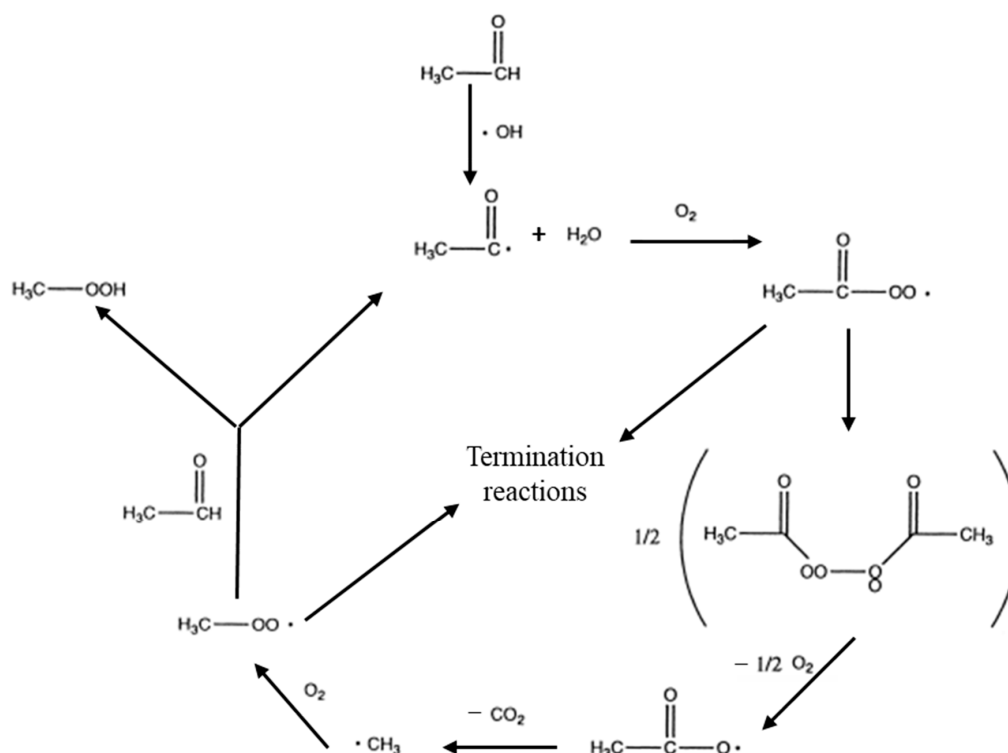


Figure 2. Schematic diagram of processes occurring during photocatalytic oxidation of acetaldehyde on an illuminated TiO_2 particle [10].

In general, the first oxidation product of acetaldehyde conversion is acetic acid, which can be mineralized to CO_2 . The remaining methyl radical is transformed into formaldehyde, which can be further oxidized to formic acid and eventually to CO_2 . The scheme of the acetaldehyde transformation on the titania surface upon UV illumination has already been reported elsewhere [11]. Below, in Figure 3, there is an outline of the path of acetaldehyde conversion by TiO_2 under weak UV illumination.

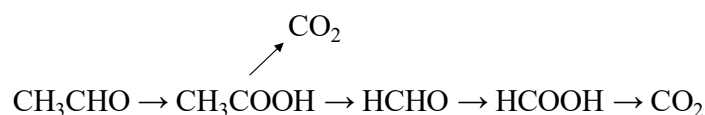


Figure 3. The proposed reaction mechanism for the photocatalytic degradation of acetaldehyde by TiO_2 under weak UV illumination [11].

Acetaldehyde can be easily decomposed to CO_2 on TiO_2 film, but some harmful byproducts such as formaldehyde are formed upon acetaldehyde conversion and can be desorbed from TiO_2 surface without further mineralization [12,13]. Although concentration of formaldehyde was observed to be not very high in the outlet gas by comparison with acetaldehyde, it was increasing with both the initial concentration of acetaldehyde and humidity of the inlet gas [12]. Higher humidity of air caused adsorption of water molecules on the titania surface in place of acetaldehyde, and then photogenerated holes were utilized in reaction with OH species rather than in oxidation of acetaldehyde. The photocatalytic conversion of acetaldehyde on TiO_2 -based materials depends on their structural parameters, phase composition and a way of chemical bonding to the surface [13–17]. Acetaldehyde is transformed through the rapid aldol condensation on the surface of anatase-type TiO_2 [18–20], whereas on the oxidized rutile (110) surface, O-acetaldehyde complexes form, which can easily undergo irreversible transformation to a highly stable surface acetate [14]. It can be a reason why the TiO_2

P25, produced by Evonik Company, which consists of both anatase (80%) and rutile (20%) phases, undergoes deactivation with time, that is contrary to anatase-type TiO₂ nanotubes [16].

The scheme of aldol condensation of acetaldehyde on titania surface is illustrated in Figure 4 [19].

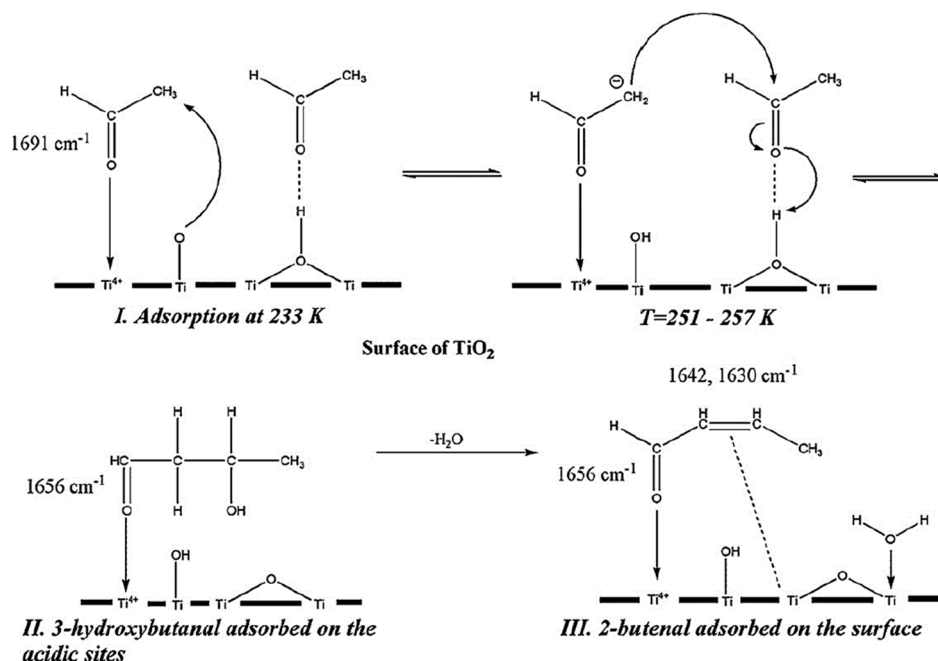


Figure 4. The schematic diagram of the proposed mechanism for the aldol condensation of acetaldehyde on TiO₂ surface. Reprinted from [19], Copyright 2020, with permission from Elsevier.

Some of the researchers proved that when acetaldehyde was brought in contact with TiO₂, it firstly adsorbed on the surface, and then an aldol condensation took place. This aldol condensation led to the formation of crotonaldehyde. At the same time, a minor fraction of acetate species was formed by oxidation processes [19].

We have proven that chemically bonded acetaldehyde with anatase surface underwent faster through photocatalytic conversion, compared to that which was weakly bonded by H-bond with OH groups [13]. Therefore, highly hydroxylated titania surface will be detrimental for the photocatalytic decomposition of acetaldehyde [13,21,22]. It was proven that adsorption of acetaldehyde in the conditions of high humidity was going through the weak physical bounding with OH groups and it was completely reversible [20]. Under UV irradiation, hydrophilicity of titania surface increases and water molecules compete with acetaldehyde to the adsorption sites of TiO₂ [23]. Therefore, photocatalytic decomposition of acetaldehyde on TiO₂ surface in the conditions of high humidity is usually lower than in dry air [11,12]. In Figure 5, the reversible adsorption of acetaldehyde in the conditions of dry air and high humidity (50%) is shown [20].

From Figure 5, it can be observed that the reversible quantity (q_{rev}) of acetaldehyde in dry air was around 3 times higher than in the conditions of high relative humidity (RH = 50%).

In this paper, there is an overview of the numerous achievements related to the application of TiO₂-based materials for acetaldehyde decomposition under different experimental conditions and various sources of light, used for the photocatalyst activation. Some of the new data were added, which complement this review in the context of the way of interaction between acetaldehyde molecules and different structures of TiO₂ surface.

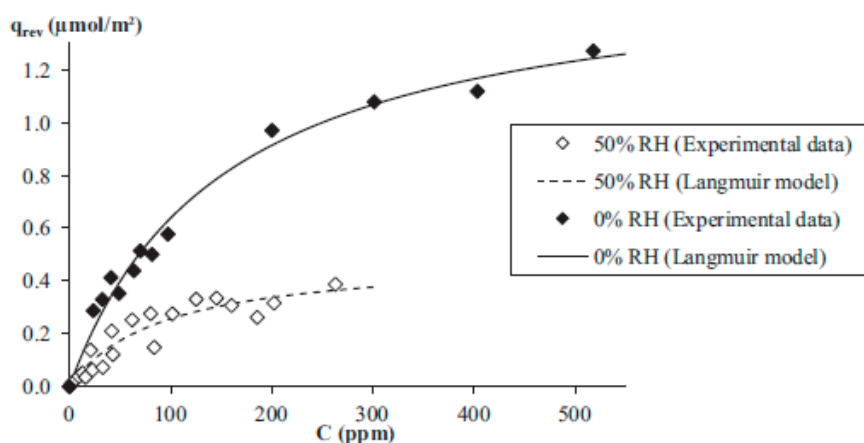


Figure 5. Acetaldehyde reversible adsorption on P25 TiO₂ isotherm under dry and humid conditions, at 23 °C. Reprinted from [20], Copyright 2020, with permission from Elsevier.

2. Preparation of TiO₂ and Impact of Its Structural Properties on Acetaldehyde Decomposition

TiO₂ is industrially produced, mainly as a white pigment, for application as an additive in paints, varnishes, plastics, sunscreens, papers, toothpastes or other materials. For large production of TiO₂, both sulphate and chloride technologies are mainly used for the final product of rutile. However, for the photocatalytic processes, nanocrystalline anatase is required, therefore the other methods are applied. The commonly used photocatalytic TiO₂, Aeroxide P25, is produced by Evonik Company by a flame method. This TiO₂ reveals relatively high BET (Brunauer–Emmett–Teller) surface area and consists of mixed phases, anatase (80%) and rutile (20%). For production of nanosized TiO₂, several other methods were developed, including: hydrothermal [24], sol-gel [25], chemical vapor deposition (CVD) [26], solvothermal [27], flame spray pyrolysis [28], electrochemical [29], microemulsion [30], micelle and inverse micelle methods [31], sonochemical reactions [32] and plasma evaporation [33]. Among all the mentioned methods, the most used are sol-gel and hydrothermal routes. The advantage of these methods relies on their flexibility to control morphology, particle size and crystallinity of the products. In the photocatalytic degradation of acetaldehyde, the mixture of anatase and brookite appeared to be advantageous [33–35]. Titania with mixed anatase and brookite was prepared by a sol-gel method from titanium isopropoxide solution and addition of alcohol with subsequent calcination at low temperatures, 200 or 450 °C [34,35]. It was proven that the presence of mixed phases anatase and brookite enhanced the density of electron traps due to the photoinduced interphase electron transfer and thereby improved photocatalytic performance of TiO₂ [35]. In Figure 6, decomposition of acetaldehyde with initial concentration around 1800 ppm in the circulated flow reactor under UV is illustrated. The samples were prepared by the sol-gel method from tetraisopropoxide solution with addition of ethanol at the different pH: 3, 10 and neutral. For acid and alkalic pH, the acetic acid and ammonia solution were used, respectively. The samples were calcinated at 400 °C. At the presence of the ammonia solution, N-TiO₂ was formed, whereas at the neutral pH, TiO₂ of mixed phases, anatase and brookite, was obtained [35]. Table 1 shows the physicochemical properties of samples [35].

It was evidenced that in case of both titania, anatase/brookite and that doped with nitrogen, the electron trap densities were higher in comparison with that of single anatase phase, as it was shown in Figure 7.

N-TiO₂ revealed higher density of electron traps than TiO₂ consisting of mixed phases of anatase and brookite, however its photocatalytic activity towards acetaldehyde decomposition was lower. The reason for that was formation of Ti³⁺ centers and oxygen vacancies in N-TiO₂, which were detrimental for acetaldehyde decomposition [35]. The most probable at the presence of oxygen vacancies, adsorption of acetaldehyde molecules on titania surface is quite different than in case of stoichiometric TiO₂ and its photocatalytic transformation towards complete mineralization is slower.

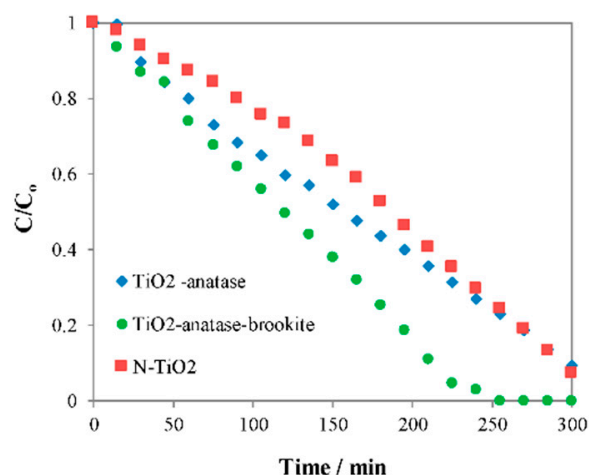


Figure 6. Photocatalytic decomposition of acetaldehyde in the circulated flow reactor under UV irradiation on TiO₂ samples prepared by a sol-gel method, the initial concentration of acetaldehyde was around 1800 ppm [35].

Table 1. Characteristics of the samples prepared by a sol-gel method [35].

Sample Name	BET Surface Area (m ² /g)	Phase Composition		Average Crystallites Size (nm)
		A—Anatase	B—Brookite	
Anatase-TiO ₂	140	A		8.7
Anatase/Brookite-TiO ₂	124	B (27%)	A (73%)	B (7.8) A (8.9)
N-TiO ₂	74	A		27.0

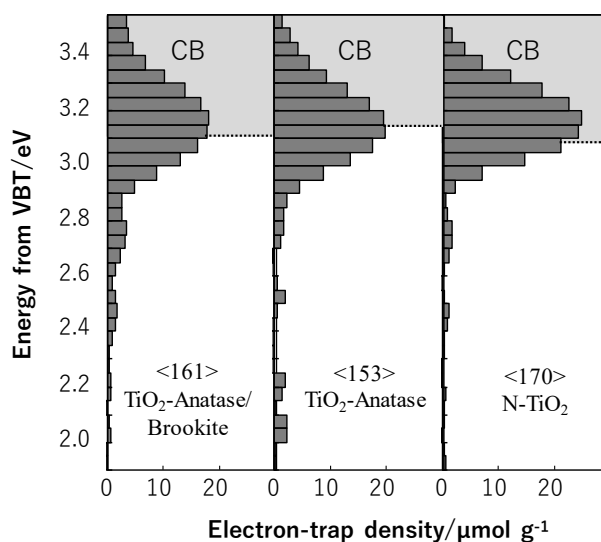


Figure 7. Electron trap densities of TiO₂ samples prepared by the sol-gel method and calcinated at 400 °C [35].

The brookite phase can also be obtained by the hydrothermal method, anodization of titanium foil or long-time grinding of anatase sample, which was previously heated at 600 °C for a few hours [36]. The solution plasma treatment of anatase can also lead to phase transformation of anatase to brookite [33]. Moreover, solution plasma treatment of TiO₂ resulted in the formation of some oxygen surface defects, however Ti³⁺ centers were not formed [33]. Both oxygen surface defects and mixture

of anatase and brookite improved charge separation in the titania sample [33–35]. Prepared in such a way, TiO₂ showed high activity towards acetaldehyde decomposition under both UV and visible light. Visible light activity of this TiO₂ was even higher than that prepared by nitrogen doping [33]. Figure 8 shows conversion of acetaldehyde towards CO₂ on the different TiO₂ samples before and after the solution plasma process (SPP), and N-TiO₂ was added for comparison [33].

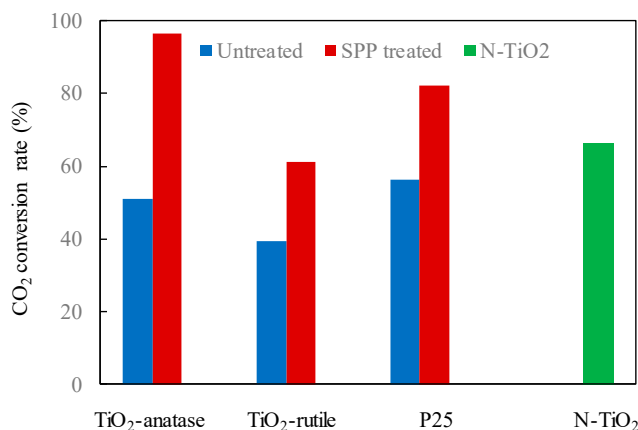


Figure 8. Quantitative comparison of CO₂ conversion rate (%) from the photocatalytic acetaldehyde degradation experiments using different photocatalyst samples [33].

The other researchers reported that Ti³⁺ defects, which were formed upon doping of carbon quantum dots, could improve separation of free charges and enhance photocatalytic decomposition of acetaldehyde [37]. However, the observed effect of enhanced photocatalytic activity was caused by the increased yield in formation of superoxide radicals rather than quantity of Ti³⁺ species. Moreover, formation of Ti³⁺ was caused not by the reducing titania itself but through the interaction of carbon quantum dots (CQDs) with TiO₂ surface. It was reported that in the CQDs/TiO₂ composite, the CQDs were grafted onto TiO₂ via Ti-O-C bond, and some delocalized electrons of CQDs migrated to TiO₂ due to the work function difference, resulting in the generation of Ti³⁺ defects in the TiO₂ matrix and positively charged surface environment of CQDs. The CQDs could promote the composites to adsorb organic compounds, improving the contact with target gas and further benefitting the photo-degradation process [37].

The great role of superoxide radicals in acetaldehyde decomposition was revealed in the literature, while the meaning of hydroxyl radicals was discounted [14,33,37]. It was widely reported in the literature, that for the efficient acetaldehyde decomposition, anatase-type TiO₂ is more active than rutile [38]. Therefore, a lot of methods of TiO₂ preparation were focused on obtaining TiO₂ with anatase structure, having relatively high BET surface area and high crystallinity [38–40]. In the sol-gel method, titanium alkoxide is usually used as a precursor and hydrolysis is accelerated by the use of acidic conditions or sonication [21]. The optimal temperature of calcination is around 400–450 °C [20,21,38,39]. Above this temperature, the anatase crystallites grow rapidly and BET surface area significantly decreases [20,25]. The sol-gel technique is also used for coating TiO₂ on various substrates in the form of a thin film [41]. It is worth to mention that some glass-coating techniques, such as dip-coating, spray-coating or spin-coating, often require to use the process of post-annealing for the crystallization into anatase structure. Post-annealing at temperatures above 450 °C causes the sodium ion diffusion from window glass into TiO₂ film and results in the decrease of the photocatalytic efficiency [26]. Therefore, the other techniques, which do not require to use the heat treatment after coating, such as CVD, spray pyrolysis or atomic layer deposition, will be more advantageous [26,28,42,43]. Some textural properties of TiO₂ can also be designed by using the template technique, solvent evaporation or an addition of a chemical agent for surface modification, such as polyethylene glycol, for example [39,43,44]. It was reported that mesoporous structure of

titania, which possessed a homogeneous pore diameter of about 6.0 nm and 11.0 nm crystalline anatase pore wall, as well as large surface area of 117 m²/g, was the most active for acetaldehyde decomposition among the other prepared samples [39]. Nanostructural TiO₂ can be obtained by the hydrothermal or electrochemical methods [15,29,45]. Titania nanotubes (TNT) of anatase structure can be obtained by the hydrothermal treatment of titania solution in an alkalic pH with addition of sodium hydroxide [45,46]. However, vertically oriented nanotubes are prepared by electrochemical anodization of titanium foil, plate or wires [15,29,47–49]. The length and the diameter of nanotubes can be controlled by the voltage, current density, anodization time and electrolyte used. In the case of the photocatalytic decomposition of toluene, the most active TNTs were obtained in ethylene glycol-based electrolyte by applying voltage of 40 V, followed by 1 h calcination at 450 °C [49]. Other authors reported that photocatalytic activity of ordered TNTs towards acetaldehyde decomposition could be enhanced by increasing their length, and they found optimum length of around 17 μm [16]. They reported that highly ordered TiO₂ nanotube array presents a porous surface and straight channels, which allow free exchange of intermediate molecules with air and/or acetaldehyde molecules. This favorable gas-phase exchange can restrain the accumulation of intermediates on the photocatalyst surface and alleviate the deactivation of nanotube arrays. They also emphasized that TiO₂ nanoparticulate film is disordered and consists of randomly packed and interconnected nanoparticles, which results in tortuous channels for the diffusion of intermediates, air and/or acetaldehyde. Therefore, compared to nanotube arrays, more intermediates can accumulate on the surface of TiO₂ nanoparticles and deactivate this photocatalyst. As a consequence, higher mineralization degree during acetaldehyde decomposition was obtained on ordered TNTs in comparison with titania film of the same thickness. In Figure 9, the SEM (Scanning Electron Microscope) images of the prepared TNTs by anodization of titanium foil are presented [16].

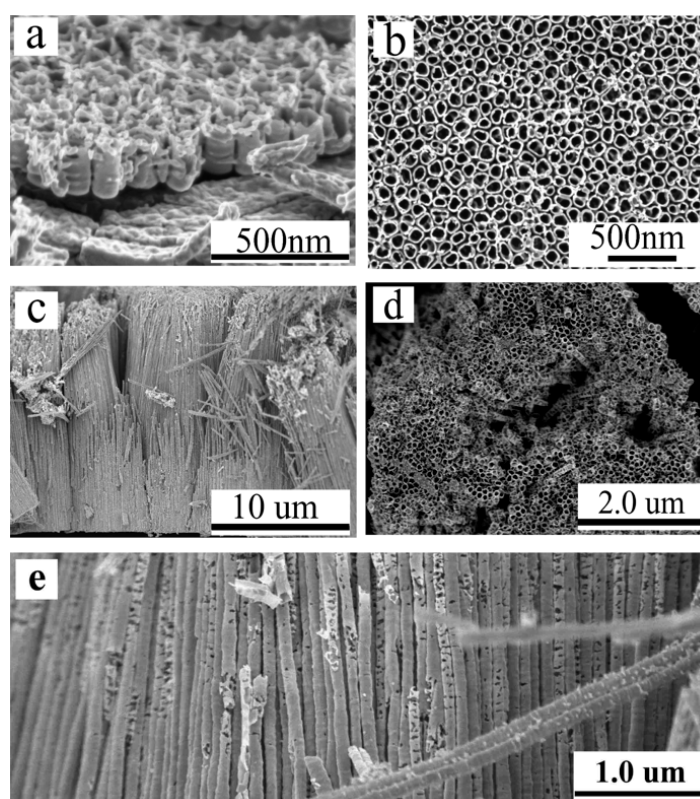


Figure 9. Cross-sectional and top-view images of TiO₂ nanotube arrays prepared by anodizing Ti foil at 20 V in 0.5 wt.% HF (Hydrofluoric Acid) aqueous solution for 20 min (a,b) and in formamide-based electrolyte for 6 h (c–e). Reprinted from [16], Copyright 2020, American Chemical Society.

It is worth mentioning that Ti nanotubes' high length, such as 17 μm , were obtained only in a formamide-based electrolyte. In Figure 10, the kinetics of the photocatalytic degradation of acetaldehyde by TiO_2 nanotube arrays is illustrated.

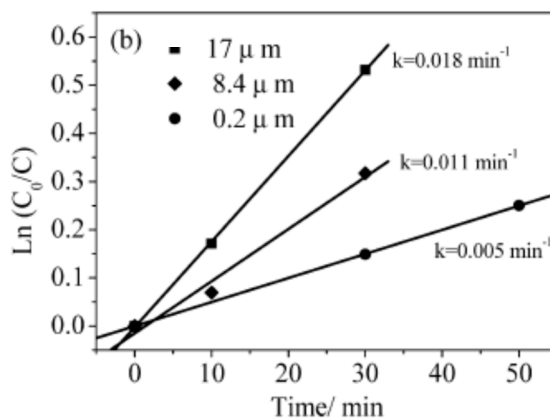


Figure 10. Dependence of $\ln(C_0/C)$ on irradiation time for the photocatalytic degradation of acetaldehyde by TiO_2 nanotube arrays with lengths of 0.2, 8.4 and 17 μm . Reprinted from [16], Copyright 2020, American Chemical Society.

Pichat previously reported that the average ratio of the efficacy of titania nanotubes (TNTs) over that of TiO_2 P25 for removal of toluene and acetaldehyde was 1.5 [50]. He assumed that preparation of TNTs by anodic oxidation could give the photocatalytic material of better performance compared to the TNT of disordered structure [50]. The other nanostructures of TiO_2 such as nanorods, nanowires or nanofibers can also be prepared by the hydrothermal method, however there are still not many studies referring to their application in the air purification systems [51–53]. It was reported that modification of titania nanostructures, such as hydrogenation of nanorods or deposition of Au on titania nanofibers, could enhance their photocatalytic activity during decomposition of acetaldehyde [52,53]. There are also some studies performed for acetaldehyde adsorption on titania nanorods of anatase structure [54]. These studies indicated that adsorption of acetaldehyde depended greatly on the partial pressure of acetaldehyde gas. For low partial pressure values, acetaldehyde was poorly adsorbed on the titania nanorods surface and this adsorption was reversible, whereas above partial pressures of 10^{-4} Torr, 96% of surface-bound acetaldehyde was chemisorbed. According to others [54], chemisorbed acetaldehyde was converted to 3-hydroxybutanal, acetate and crotonaldehyde. Low and reversible adsorption of acetaldehyde on titania nanorods can limit its application in the photocatalytic processes. However efficient decomposition of acetaldehyde was reported over brookite TiO_2 nanorods, which were prepared by the hydrothermal method [55]. The photocatalytic activity for decomposition of acetaldehyde increased with an increase in the aspect ratio of (2 1 0) to (2 1 2) exposed crystal faces, which were attributed to reduction and oxidation sites, respectively. Site-selective Fe^{3+} modification of brookite nanorods enhanced its photocatalytic activity [55]. Dependence of the exposed anatase crystal faces on the photocatalytic decomposition of acetaldehyde was reported by another research group [17]. Titania films with a large fraction of exposed anatase (001) facets exhibited higher activity towards acetaldehyde decomposition than those exposing predominantly (101) [17]. Ohno et al. [56] prepared TiO_2 nanorods consisting of rutile phase from TiCl_3 solution containing NaCl under hydrothermal conditions [56]. The obtained rutile fine particles showed high photocatalytic activity for degradation of 2-propanol and acetaldehyde under UV irradiation compared to the activity of other commercial anatase fine particles (ST-01) developed for environmental clean-up [56]. Their studies showed that the (110) face of rutile provides reductive sites and the (111) face has mainly oxidative sites. They concluded that the crystal faces facilitate the separation of electrons and holes,

resulting in improvement of the photocatalytic activity [56]. The role of the crystal faces of anatase and rutile in the photocatalytic reactions of oxidation and reduction was discussed elsewhere [57].

3. Adsorption of Acetaldehyde and Its Photocatalytic Transformation on TiO₂

In the photocatalytic gas-phase reactions, contact of the organic molecules with the photocatalyst surface is crucial. It was widely reported that acetaldehyde adsorbed on the anatase surface can undergo an aldol condensation to produce crotonaldehyde [11,13,18–20,58–60]. In situ FTIR (Fourier-transform infrared spectroscopy) experiments of acetaldehyde adsorption showed that acetaldehyde underwent both the aldol condensation and to a minor extent, oxidation [19]. The aldol condensation resulted in the formation of 3-hydroxybutanal and crotonaldehyde, while the oxidation processes led to formation of bidentate acetate, which was bounded to the titania surface [19]. It was also revealed that upon illumination of TiO₂ with UV light, the initially formed species were converted into several other intermediates, such as acetic acid, formic acid and formaldehyde [19]. Crotonaldehyde was photocatalytically converted to acetate and formate species. The formed formate species could be further oxidized to formic acid and eventually to CO₂ [19]. The other researchers reported that adsorption of acetaldehyde on TiO₂ depended on the exposed anatase faces [59]. The titania, with dominant anatase face (001), showed higher adsorption and photocatalytic conversion of acetaldehyde than those which had dominant faces of anatase (101) and (010) [59]. The photocatalytic conversion of flowing acetaldehyde under UV-Vis light in dependence on the dominant face of anatase is shown in Figure 11 [59].

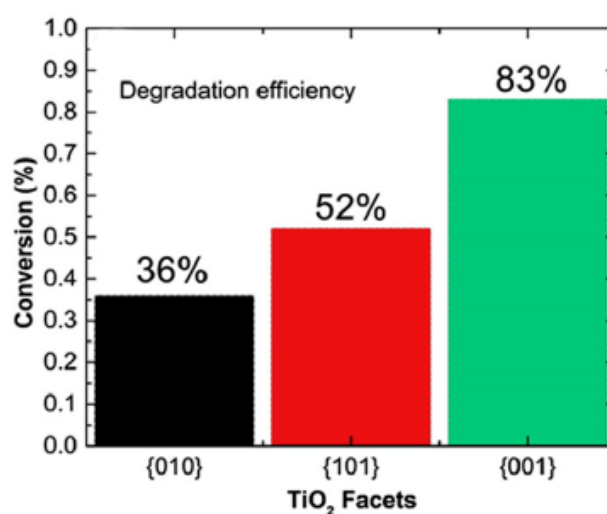


Figure 11. Degradation efficiency of gaseous acetaldehyde under UV/Vis irradiation in dependence on the dominant face of anatase type TiO₂, the flow rate = 20 sccm (standard cubic centimeters). Reprinted from [59], Copyright 2020, with permission from Elsevier.

However, a high impact of surface area on the adsorption and decomposition of acetaldehyde was also noticed. Under experimental conditions, the anatase sample with dominant (001) face showed the highest specific surface area among the others [59]. The increase of the retention time of acetaldehyde over the titania by decreasing the flow rate of gaseous acetaldehyde from 20 to 10 sccm greatly boosted its photocatalytic conversion on samples with dominant anatase faces (101) and (010), as shown in Figure 12 [59].

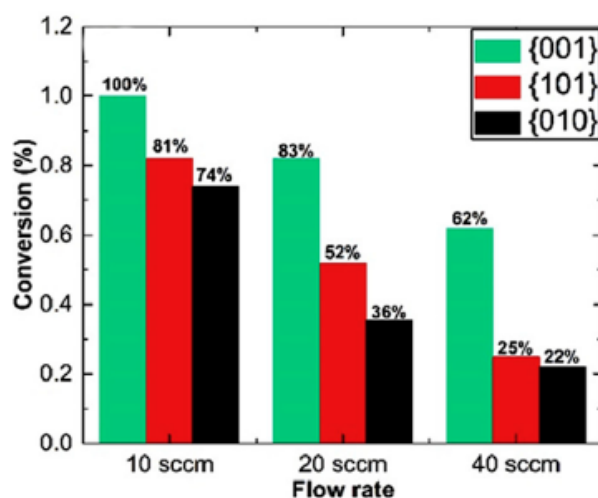


Figure 12. Degradation efficiency of gaseous acetaldehyde at different flow rates under UV/Vis irradiation on anatase type TiO_2 with different dominant faces. Reprinted from [59], Copyright 2020, with permission from Elsevier.

It means that contact time of acetaldehyde molecules with the active surface of photocatalyst is essential. If acetaldehyde is poorly adsorbed on the titania surface, the contact time of molecules with the surface should be long enough to facilitate their diffusion to the surface. Increased adsorption of acetaldehyde on the surface of titania nanorods by increasing the partial pressure of acetaldehyde gas was also reported by others [54]. Adsorption of acetaldehyde on the titania surface is essential, however, the way acetaldehyde binds with the surface seems to be crucial for its conversion by means of photocatalytic reactions. It was reported that acetaldehyde could be adsorbed either physically or chemically on the titania surface [11,13,20]. Under the humid conditions or on highly hydroxylated titania surface, acetaldehyde is mainly physisorbed with possible reversible desorption [11,13,20]. On the contrary, the chemical binding of acetaldehyde on titania surface takes place on the low hydroxylated surface and then its further conversion occurs [13]. The stability of formed intermediates on the titania surface influences the efficiency of the acetaldehyde degradation. As it was reported elsewhere [14,58], acetaldehyde was adsorbed to a higher extent on the reduced anatase and rutile than on their oxidized forms. It has been found that acetaldehyde molecules undergo adsorption preferentially via the oxygen vacancy sites in the reduced titania, followed by formation of butene complex [58]. Formation of such species is not a catalytic process. The oxygen vacancy sites are active centers in this reaction, that are consumed irreversibly and are not regenerated during the process [58]. However, on the stoichiometric and oxidized surface of rutile (110), acetaldehyde can be converted to acetate, which is stabilized on the surface and desorbs at high temperatures [58]. Such pathway of acetaldehyde conversion on rutile is accompanied by blocking of the active sites on the rutile surface. For that reason, the number of the sites decreases with time and becomes unavailable for the next molecules of acetaldehyde [58]. The adsorption of acetaldehyde on the photocatalyst surface is also influenced by the formation of active radicals. It was proven that acetaldehyde adsorption on rutile resulted in a decreasing of its efficiency for formation of hydroxyl radicals [15]. Besides that, photoluminescence spectra showed improved charge separation of free radicals on the rutile surface loaded with adsorbed acetaldehyde molecules. It was caused by the interaction of acetaldehyde molecules with the rutile surface. It was revealed that acetaldehyde acted as a donor molecule when it was adsorbed on the rutile surface [15]. However, formation of superoxide radicals on rutile with adsorbed acetaldehyde did not differ significantly in comparison with pure rutile [15]. Nevertheless, the highest decomposition of acetaldehyde on rutile was evidenced in the atmosphere consisted of nitrogen, oxygen and water vapor, but was the lowest in the absence of oxygen. It means that superoxide radicals have a dominant role in the acetaldehyde decomposition over rutile-type TiO_2 [15]. The aforementioned

facts indicate the importance of molecules' interaction with the photocatalyst surface in terms of the photocatalytic process. Therefore, we have performed new studies using different types of commercial titania samples towards their application for air purification. Adsorption capacities of acetaldehyde were determined together with the interaction of acetaldehyde molecules with titania surface. For experiments, two samples of Kronos International Ltd. (Germany) were used (KRONOClean®7000 and KRONOClean®7050), which were anatase-type TiO₂ of nanocrystalline structure. KRONOClean®7000 was modified by carbon species and was designed as a visible light photocatalyst. Additionally, some samples of Evonik Company (Germany) were also tested, P25 and P90, which consisted of both anatase and rutile structures in different ratios. For comparison, two other commercial samples of rutile structure were studied, nanocrystalline rutile produced by Sachtleben (Germany) and Tytanpol produced by Chemical Factory Azoty (Poland). The brief characteristics of these commercial samples are introduced in Table 2.

Table 2. Characteristics of commercial titanias.

Sample Name	Supplier	BET Surface Area (m ² /g)	Phase Composition (%)		Average Crystallites Size (nm)
			A-Anatase	R-Rutile C-Carbon	
KRONOClean®7050	Kronos Ltd.	322	A > 85		6.9
KRONOClean®7000	Kronos Ltd.	242	A > 87.5; C: 1		11.0
P25	Evonik	54	A: 78; R: 22		A: 21.0; R: 55
P90	Evonik	99	A: 89; R: 11		A: 29.3; R: 55.9
Nanorutile	Sachtleben	122	R: 97; A: 3		R: 14.5; A: 5.3
Tytanpol	Chemical Factory Azoty	8	R: 100		320.0

The adsorption capacity of titania samples with dominant anatase structure towards acetaldehyde was well-correlated with their specific surface area, whereas in the case of rutile-type samples, it was somewhat lower than on anatase, but was also dependent on the materials' porosity. Photocatalytic decomposition of acetaldehyde under fluorescent lamp irradiation was performed according to the procedure described elsewhere [61]. The studies of acetaldehyde decomposition (300 ppm) under the flow rate of 20 ml/min were carried out. The performed experiments showed that acetaldehyde decomposition was not dependent on the surface area of titania samples, and results are listed in Table 3. This process was conducted under continuous flow of gaseous acetaldehyde. Acetaldehyde decomposition after 10 h was listed to compare it with the CO₂ formation. After 1 h of light illumination, part of formed CO₂ was a result of decontamination of titania samples from some of the carbonaceous impurities.

Table 3. Adsorption capacities and decomposition degree of acetaldehyde on studied titanias.

Sample Name	Adsorption Capacity (mg/g)	Acetaldehyde Decomposition after 10 h (%)	CO ₂ Formation after 1 h (ppm)	CO ₂ Formation after 10 h (ppm)
KRONOClean®7050	93.5	35	245	245
KRONOClean®7000	66.6	28	220	196
P25	19.6	28	198	173
P90	37.3	35	245	245
Nanorutile	24.8	9	50	28
Tytanpol	-	3	10	0

The highest photocatalytic decomposition of acetaldehyde was noted for P90 and KRONOClean®7050 samples, whereas rutile-type TiO₂ were poorly active, regardless of their porosity. The measurements of CO₂ formation upon irradiation time showed that mineralization degree of acetaldehyde was decreasing over time for P25, KRONOClean®7000 and rutile-type samples.

To understand the mechanism of acetaldehyde conversion via the photocatalytic process, FTIR spectra of samples after adsorption and following photocatalytic decomposition were performed and illustrated in Figure 13. The samples produced by Kronos Company had higher hydroxylated surface in comparison to those obtained by Evonik. Nanorutile also has more hydroxylated surface than Tytanpol. P25, P90, KRONOClean® 7000 and nanorutile samples showed some bands of carbon species on FTIR spectra. After adsorption of acetaldehyde on titania samples, new bonds appeared, such as C=O, COO, C=C, C-H, C-C and CH₃, which were assigned to adsorbed acetaldehyde, crotonaldehyde and acetate species. The list of FTIR bands with their identification is introduced in Tables 4–8. The adsorption of acetaldehyde on TiO₂ surface differed between anatase and rutile. The bands at 1444 and 1537 cm⁻¹ assigned to COO species from CH₃COO⁻ [19] were more intensive on nanorutile and TiO₂ samples containing rutile structure. However, the bands of CH₃ species at 1333 and 1421 cm⁻¹ assigned to adsorbed CH₃COO⁻ [19] were the most intensive on Kronos samples. Most likely, the bonding of acetate species with anatase surface is different than that with rutile. The C=O bands at 1706, 1715 and 1766 cm⁻¹, assigned to HCOOH species [19], were observed after acetaldehyde adsorption on all the titania surfaces, however on rutile, they were more intensive. The band at 1351 cm⁻¹ observed on nanorutile after adsorption of acetaldehyde can be assigned to C-O species in HCOOH [62]. The band at 1633–1635 cm⁻¹ assigned to C=C vibrations in crotonaldehyde was the most intensive in titania Kronos and P90 samples, it could be connected with high adsorption of acetaldehyde on these samples and occurring aldol condensation on anatase structure. These FTIR measurements showed that acetaldehyde reacted with TiO₂ surface through the formation of crotonaldehyde and was partly oxidized to acetic and formic acids. Oxidation of acetaldehyde to acetate and formate species was carried out more efficiently on rutile than anatase, but an aldol condensation to crotonaldehyde was more efficient on anatase surface. In Figure 14, the FTIR spectra of titania samples after the photocatalytic process are shown. P25 and P90 revealed a lower intensity band at 1631 cm⁻¹ assigned to adsorbed water molecules than Kronos samples and higher intensity bands at 1412 and 1442 cm⁻¹ assigned to CH₃ species in the acetic acid and crotonaldehyde, respectively [19,62]. The bands of C=O at 1686 and 1715 cm⁻¹ assigned to CH₃COOH and HCOOH respectively, were more intensive on TiO₂ samples, which contained rutile. The highly intensive band at 1439 cm⁻¹ on nanorutile was assigned to COO vibrations in the acetic acid [11]. Tytanpol rutile showed highly intensive bands at 1718 and 1764 cm⁻¹ assigned to C=O groups in formate species. These measurements revealed that the interaction of acetaldehyde with anatase surface is quite different than that with rutile. Acetaldehyde is more favorably adsorbed on anatase, and undergoes an aldol condensation in the dark, whereas on rutile, the oxidation of acetaldehyde to acetic and formate species takes place. Under illumination of a fluorescent light, both acetic and formic acids are deposited on rutile and slow down the process of acetaldehyde decomposition. A similar effect was noted by other researchers [62], who observed that deposition of formic acid on TiO₂ during acetaldehyde decomposition deactivated its surface. After the photocatalytic process, the amount of both the acetic and formic acids adsorbed on titania surface was higher on rutile than anatase-type samples, most probably, they were poorly mineralized on rutile. It can be concluded that rutile oxidizes acetaldehyde at the presence of oxygen easier than anatase. The products of acetaldehyde oxidation are deposited on TiO₂ surface and slow down the process of its further decomposition. The scheme illustrating transformation of acetaldehyde on anatase and rutile surfaces under dark conditions and after illumination with weak UV light is shown in Figure 15. Other researchers investigated the photocatalytic properties of nanorutile, and they proved that rutile was a material of more reductive properties than anatase and was able to adsorb more oxygen [63]. It was also proven that oxygen could react with adsorbed acetaldehyde at low temperature and oxidize it to the acetic acid [64]. Such pathway of acetaldehyde conversion on TiO₂ surface appeared to be less efficient, because acetic acid deposited on TiO₂ was stable and its further decomposition was limited [15]. It is worth mentioning that during acetaldehyde decomposition, acetic acid was detected in the outlet stream of the acetaldehyde gas. The concentration of acetic acid was increasing with time during adsorption in the dark for all types of TiO₂, but after the lamp was

switched on, this concentration was decreasing for anatase-type samples and increasing for rutile. It means that proceeding photocatalytic reactions on anatase could mineralize acetic acid more efficiently than those occurring on rutile.

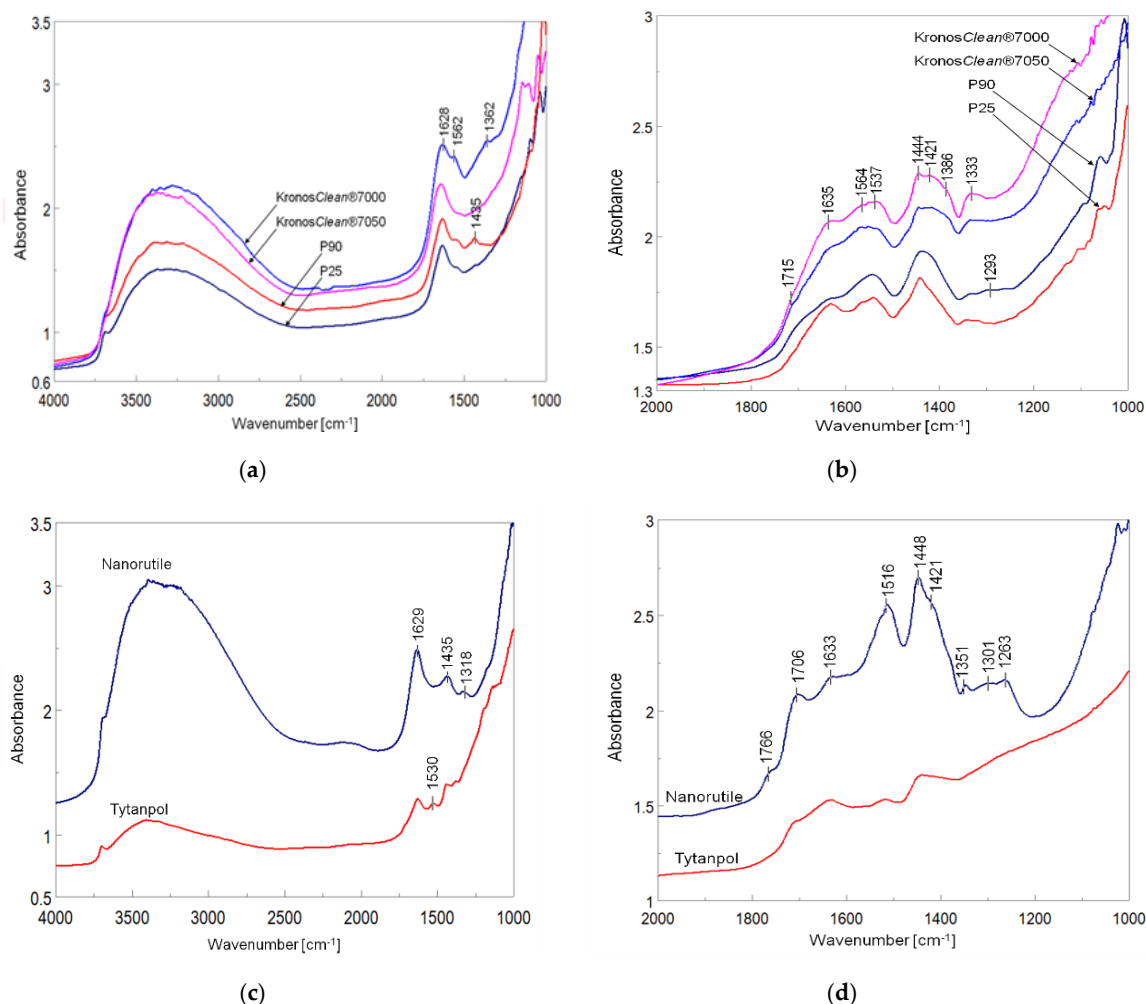


Figure 13. FTIR spectra of titania Kronos and Evonik samples as received (a) and after adsorption of acetaldehyde (b), rutile samples as original (c) and after adsorption of acetaldehyde (d).

Table 4. Assignment of FTIR bands observed for commercial titania samples, as received.

Vibration Mode	Wavenumber (cm ⁻¹)	
	This Article	Literature
<i>d</i> (OH)	1629	1620/1630 [25]
<i>n_{as}</i> (COO)	1562	1562 [11,19]
<i>n_{as}</i> (COO)	1530	1532 [25]
<i>d</i> (CH ₃)	1435	1437 [11]
<i>d</i> (CH)	1362	1361 [19]
<i>d</i> (CH ₃)	1318	1313 [62]

Table 5. Assignment of FTIR bands observed for commercial titania samples (P25, P90, KronosClean®7000 and KronosClean®7050) after adsorption of acetaldehyde.

Molecule	Wavenumber (cm ⁻¹)		
	Vibration Mode	This Article	Literature
HCOOH	<i>n</i> (C=O)	1715	1706 [19]
CH ₃ (CH) ₂ CHO	<i>n</i> (C=C)	1635	1628 [19]
HCOO ⁻	<i>n_{as}</i> (COO)	1564	1560 [19]
CH ₃ COO ⁻	<i>n_{as}</i> (COO)	1537	1540 [19]
CH ₃ COO ⁻	<i>n_s</i> (COO)	1444	1444 [11]
CH ₃ COO ⁻	<i>d</i> (CH ₃)	1421	1422 [19]
HCOO ⁻	<i>d</i> (CH)	1386	1380 [19]
CH ₃ COO ⁻	<i>d_{as}</i> (CH ₃)	1333	1338 [19]
CH ₃ COOH	<i>n</i> (C-O)	1293	1294 [19]

Table 6. Assignment of FTIR bands observed for commercial rutile-type titania samples after adsorption of acetaldehyde.

Molecule	Wavenumber (cm ⁻¹)		
	Vibration Mode	This Article	Literature
HCOOH	(C=O)	1766	1776 [19]
HCOOH	(C=O)	1706	1706 [19]
CH ₃ (CH) ₂ CHO	(C=C)	1633	1628 [19,62]
unknown	-	1516	-
CH ₃ COO ⁻	<i>s</i> (COO)	1448	1444 [11]
CH ₃ COO ⁻	(CH ₃)	1421	1420 [19]
HCOO ⁻	<i>s</i> (C-O)	1351	1355 [62]
HCHO	(CH ₂)	1301	1302 [19]
HCHO	(CH ₂)	1263	1251 [19]

Table 7. Assignment of FTIR bands observed for commercial titania samples (P25, P90, KronosClean®7000 and KronosClean®7000) after photocatalytic decomposition of acetaldehyde.

Molecule	Wavenumber (cm ⁻¹)		
	Vibration Mode	This Article	Literature
HCOOH	(C=O)	1717	1713 [19]
HCOOH	(C=O)	1715	1713 [19]
CH ₃ COOH	(C=O)	1686	1675 [19]
H ₂ O	(H ₂ O)	1631	1620/1630 [25]
HCOO ⁻	<i>as</i> (COO)	1561	1560 [19]
CH ₃ COO ⁻	<i>as</i> (COO)	1526	1540 [19]
CH ₃ (CH) ₂ CHO	<i>as</i> (CH ₃)	1442	1442 [19]
CH ₃ COOH	(CH ₃)	1412	1415 [19]
HCOO ⁻	(CH)	1384	1380 [19]
CH ₃ COO ⁻	<i>as</i> (CH ₃)	1334	1338 [19]
CH ₃ COOH	(C-O)	1273	1293 [19]
CH ₃ (CH) ₂ CHO	(C-C)	1173	1168 [62]

Table 8. Assignment of FTIR bands observed for commercial rutile-type titania samples after photocatalytic decomposition of acetaldehyde.

Molecule	Wavenumber (cm ⁻¹)		
	Vibration Mode	This Article	Literature
HCOOH	(C=O)	1764	1776 [19]
HCOOH	(C=O)	1718	1713 [19]
Ti-OH	(OH)	1629	1620/1630 [25]
unknown	-	1515	-
CH ₃ COO ⁻	<i>s</i> (COO)	1439	1436/1444 [11]
HCOO ⁻	<i>s</i> (C-O)	1351	1355

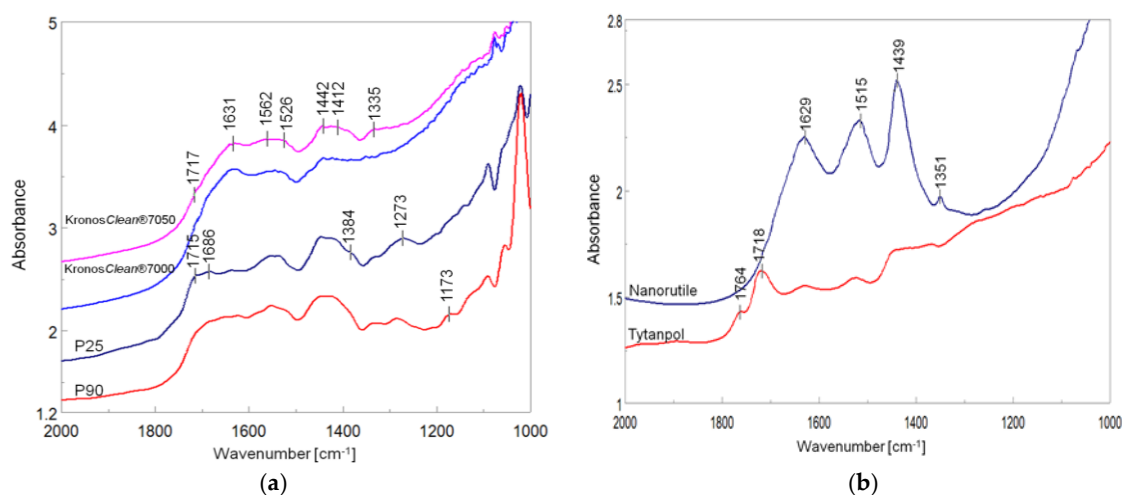


Figure 14. FTIR spectra of titania samples after photocatalytic decomposition of acetaldehyde, (a) Kronos and Evonik and (b) rutile.

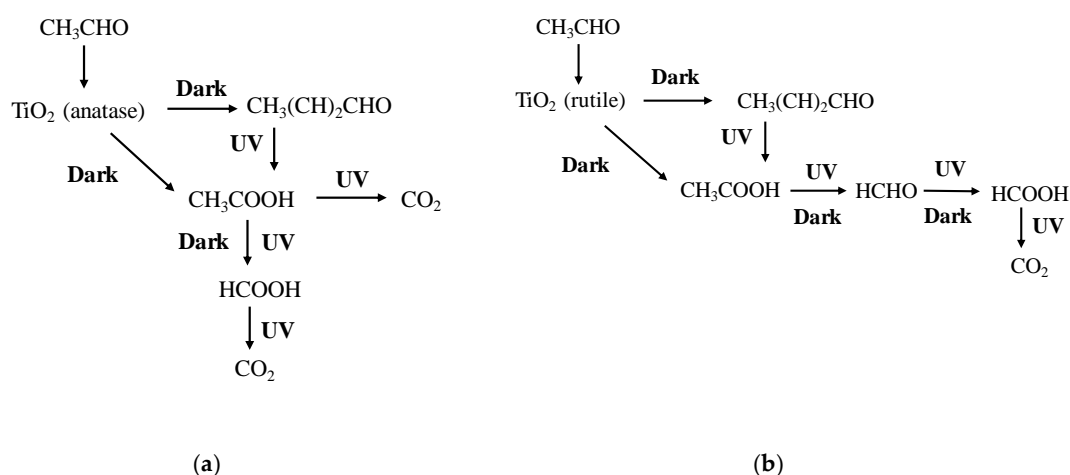


Figure 15. Scheme of the acetaldehyde conversion on titania surface during adsorption in the dark and photocatalytic decomposition under weak UV irradiation: (a) anatase, (b) rutile.

To summarize the impact of acetaldehyde adsorption on titania surface for its further conversion during photocatalytic process, it can be concluded that the chemical bonding of acetaldehyde with TiO_2 surface is essential and depends on its crystalline structure. Low hydroxylated anatase surface can easily adsorb acetaldehyde by the chemical way through the aldol condensation to crotonaldehyde. Such adsorbed molecules can undergo further transformation via the photocatalytic process, leading to formation of acetate, formaldehyde, formate species and CO_2 . Conversion of acetaldehyde on rutile-type surface conducts fast oxidation of acetaldehyde to stable-surface acetate species, which limits its further decomposition. Geometry of the crystalline structure of anatase and rutile influences the quantity of acetaldehyde adsorption. Anatase with dominant (001) face and both reduced anatase (001) and reduced rutile with dominant (110) face showed enhanced adsorption of acetaldehyde [14,17,58]. However, adsorption of acetaldehyde on the reduced defect sites of TiO_2 conducts irreversible utilization of these active sites, so it can improve the adsorption abilities of TiO_2 up to saturation of oxygen vacancies. Nevertheless, exposition of reduced titania surface to acetaldehyde gas for a long period of time can partly deactivate its surface.

4. The Role of Reactive Oxygen Radicals in the Photocatalytic Conversion of Acetaldehyde

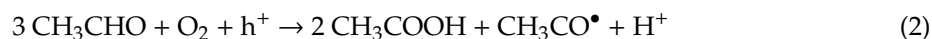
Various potential pathways for the photocatalytic degradation by TiO₂ have been proposed, including action of reactive species such as: hydroxyl radicals, carbonyl radicals, superoxide radicals and hydrogen peroxide [33].

Other studies concerned a general mechanistic way of acetaldehyde decomposition through its conversion to acetate, and then to formaldehyde, followed by transformation of the latter to formates and finally to CO₂ [11]. However, both interaction of acetaldehyde with the reactive surface and formed oxygen radicals may reveal an impact on the reaction pathway. Transformation of acetaldehyde to crotonaldehyde and its partial oxidation to acetic acid on anatase surface was confirmed by many researchers [11,19,20]. Impact of oxygen on the oxidation and decomposition of acetaldehyde was also recognized and reported [10,11]. The mechanism of acetaldehyde decomposition via radical-initiated chain reactions consuming oxygen was also proposed [10]. It was evidenced [15] that acetaldehyde adsorbed on rutile-type TiO₂ significantly limited the extent of hydroxyl radicals' formation, but at the same time, was recognized as neutral for the formation of oxygen superoxide species. In addition, a great role of superoxide radicals in the photocatalytic decomposition of acetaldehyde on rutile was reported [15]. Other researchers also postulated that efficient decomposition of acetaldehyde could be achieved in the presence of formed O₂^{-•} species [33]. The authors reported that oxygen vacancies formed upon the solution plasma process and surface defects below the conduction band in TiO₂, were capable to accelerate formation of reactive species [33]. These defects attracted atmospheric oxygen, and converted it to O₂^{-•}, as illustrated by reaction scheme (1).

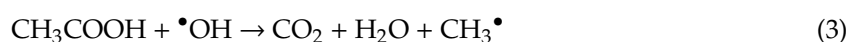
Photogenerated electrons take part in the following reaction:



Whereas formed holes (h⁺) mediate in the reaction of carbonyl radicals' formation:



The carbonyl radicals (CH₃CO[•]) are capable to react with O₂, which mediates the chain reactions of acetaldehyde oxidation. In these multiple reactions, acetic acid is the main intermediate in the transformation of acetaldehyde to CO₂, according to the reaction [33]:



Therefore, the improved separation of free radicals formed in TiO₂ can conduct enhanced photocatalytic conversion of acetaldehyde. The improvement in charge separation can be achieved by mixing of two different TiO₂ phases—either brookite with anatase or anatase with rutile [34,35], or by the synthesis of TiO₂ consisting of the proper ratio of the oxidative and reductive centers [12,17,55–57,59]. This effect can be realized for example by increasing the share of anatase (001) face of in the synthesized titania [17].

Formation of both types of radicals, O₂^{-•} and [•]OH, is demanded for complete decomposition of acetaldehyde. The main route of [•]OH formation includes action of the photogenerated holes:

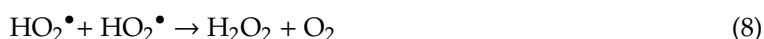


Other options of hydroxyl radicals' generation are illustrated by reaction schemes (5) and (6):



According to Zeng et al. [15], high yield of acetaldehyde decomposition on rutile was observed under atmosphere of nitrogen, oxygen and water vapor [15]. However, due to the competition between acetaldehyde and water to the adsorption sites of TiO₂, the presence of water may suppress acetaldehyde decomposition on TiO₂ [11,20]. Compared to anatase, the ability of rutile to form hydroxyl radicals is poor. Nevertheless, the formation of a high quantity of •OH radicals on rutile was confirmed in the presence of H₂O₂. It was proven [64] that O₂^{•-} radicals formed on the surface of nanosized rutile reduced H₂O₂ to •OH, according to the reaction (6).

The pathways of H₂O₂ formation during photocatalytic processes occurring on TiO₂ are illustrated by reaction schemes (7)–(10):



It is assumed that poor photocatalytic activity of rutile in comparison with anatase could be caused by high transformation of acetaldehyde to both acetic and formic acids, and by the high stability of the acetate species on rutile surface. On the contrary, adsorption of acetaldehyde on anatase TiO₂ was proceeded greatly through an aldol condensation to crotonaldehyde. Under UV irradiation, crotonaldehyde was either oxidized to acetate and formate species or directly mineralized to CO₂. Such pathway of acetaldehyde decomposition on anatase was more efficient in the formation of CO₂ than that on rutile. Undoubtedly, oxygen takes part in the photocatalytic oxidation of acetaldehyde and it is consumed during photocatalytic chain reactions. Interestingly, it was reported that in the absence of gaseous oxygen, surface-adsorbed oxygen was consumed during the formation of the acetate and the formate. However, if the adsorbed O₂ was consumed in the process, only minor amounts of acetaldehyde were decomposed into the formate [11]. After the photocatalytic process of acetaldehyde decomposition, the rutile type of TiO₂ indicated some content of formate species adsorbed on the surface. The amount of formate species formed was much higher on rutile than on anatase surface samples (Figure 14). This implies that oxygen adsorbs on rutile surface more efficiently than on anatase, and this adsorbed oxygen takes part in the oxidation of acetate species. Nevertheless, rutile is less efficient in mineralization of acetic acid than anatase-type TiO₂.

5. The Impact of Light Wavelength Region on the Photocatalytic Decomposition of Acetaldehyde

The efficiency of the photocatalytic reactions depends on the energy of the incident photons. However, even a few photons of the required energy can induce the photocatalytic process. As reported by Fujishima et al. [10], in a well-lit room with the total light intensity of 10 μW/cm² (1 μW/cm² of UV needed to excite TiO₂), the energy of photons would be sufficient enough to decompose a hydrocarbon layer of approximately 1 μm thick every hour [10]. Therefore, they recommended to use a fluorescent light as a source capable to induce photocatalytic decomposition of VOCs on TiO₂. The studies, conducted by different teams, indicated that acetaldehyde was successfully undergoing photocatalytic decomposition on TiO₂ surface under light emitted by the fluorescent lamps. However, efficiency of this process was lower than under UV-A light generated by a typical UV lamp [12,33,61]. To increase utilization of solar light, a lot of recent studies have been focused on the preparation and examination of visible-light active photocatalysts. One of the first works on the activity of nitrogen-doped TiO₂ towards acetaldehyde decomposition under visible light was reported by Asahi et al. in *Science Journal* [65]. They prepared TiO_{2-x}N_x films by sputtering the TiO₂ target in an N₂ (40%)/Ar gas mixture followed by annealing at 550 °C in N₂ gas. The obtained nitrogen-doped TiO₂ film showed absorption of visible light of a wavelength below 500 nm and the photocatalytic degradation of acetaldehyde for λ = 435 nm. The activities of both TiO₂ films, doped with nitrogen and undoped, under UV light were comparable and higher than under visible light irradiation. The results are illustrated in Figure 16 [65].

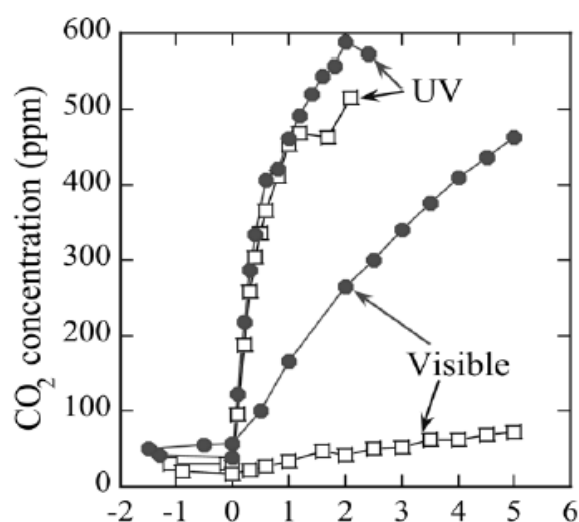


Figure 16. CO₂ evolution as a function of irradiation time (light on at zero) during the photodegradation of acetaldehyde gas (with an initial concentration of 485 ppm) under UV and visible light irradiation; TiO_{2-x}N_x = solid circles, TiO₂ = open squares. From [65]. Reprinted with permission from AAAS, Copyright 2020.

After publishing Asahi's findings [65], numerous research works were targeted to obtain the visible light active TiO₂ through doping of different anionic species, such as N, C, S and F as single doping or co-doped [37,66–71], also with some metallic species such as Au, Ag, Cu, Co, Pt, Mn, Fe and others [72–79]. The composites of TiO₂ with other metal oxides such as WO₃ or CeO₂ were also prepared and showed photocatalytic activity under visible light irradiation towards acetaldehyde decomposition [80,81]. An activity of doped TiO₂ under visible light was mainly obtained due to either the narrowing of the band gap in TiO₂ [65,66,69] or by the introduction of an impurity level of dopant inside the titania structure and formation of intra-band-gap energy levels [77]. Formation of surface defects in TiO₂ was also reported [33] as resulting in increasing the activity of titania under visible light. Nitrogen doped to TiO₂ can be localized at the interstitial or substituted position. Asahi et al. [65] reported that in the anatase-type TiO₂, oxygen atoms are substituted by nitrogen ones, causing mixing of O2p and N2p states and narrowing of the titania band gap. However, the other researchers stated that by substitutional doping of nitrogen to TiO₂, some localized impurity states are formed just above the valence band of TiO₂ without mixing of N2p and O2p states [82]. Moreover, they claimed that nitrogen builds into the titania lattice in the interstitial position and forms localized energy levels in the form of NO bonds [82]. The authors did not confirm the narrowing of the band gap, but such interstitial doped nitrogen caused activity of TiO₂ in the range of visible light [82]. Such observation was also confirmed by Meroni et al. [66] and Sakatani et al. [83], who reported that the interstitially doped nitrogen and concentration of the paramagnetic centers in nitrogen-doped TiO₂ seemed to control the absorption of visible light and the activity of titania samples. Similar results were reported by our research group [61]. Generally, it is accepted that nitrogen doped to TiO₂ increases absorption of light to the visible region. However, photocatalytic activity of TiO₂ modified in such a way depends on its electronic structure, rather than the ability for visible light absorption [33,61,66]. Fujishima et al. [33] reported that although samples of TiO₂ prepared through the solution plasma process indicated absorption of visible light, their photocatalytic activity towards acetaldehyde decomposition was governed mainly by the intensity of UV light, with a wavelength below 400 nm. The solution plasma process caused formation of surface defects in TiO₂, which were most likely responsible for its enhanced photocatalytic activity. Nitrogen doping to TiO₂ also generates some oxygen vacancies and surface defects, however the superiority of TiO₂ modified by solution plasma process over the N-doped TiO₂ in the photocatalytic decomposition of acetaldehyde was demonstrated [33]. Meroni et al. [66]

also indicated the poor activity of N-doped TiO₂ under visible light towards acetaldehyde decomposition, compared to the effect achieved under UV or UV-Vis. Doping of some species to TiO₂ can retard charge separation and enhance its photocatalytic activity through the formation of different surface defects. Higher density of electron traps was measured in N-doped TiO₂ in comparison with the undoped one, however photocatalytic decomposition of acetaldehyde under irradiation of a fluorescent lamp was more efficient for TiO₂ itself [61]. The presence of Ti³⁺ surface defects in N-TiO₂ appeared to be detrimental in acetaldehyde decomposition [61]. It is worth mentioning that the solution plasma process did not cause formation of Ti³⁺ centers in TiO₂ [33]. Co-doping of anionic or anionic/metallic species to TiO₂ can increase both the amount and type of active sites, which conducts successful narrowing of the band gap, suppresses the recombination process between photoinduced pairs of h⁺/e⁻ and increases its photocatalytic activity [69,72–74,79]. As reported elsewhere [72–74], different oxidation states of metals are responsible for charge trapping and improved charge separation [72–74]. Synergistic effects of co-dopants (nitrogen and platinum species) were reported by Kim et al. [74] and illustrated in Figure 17.

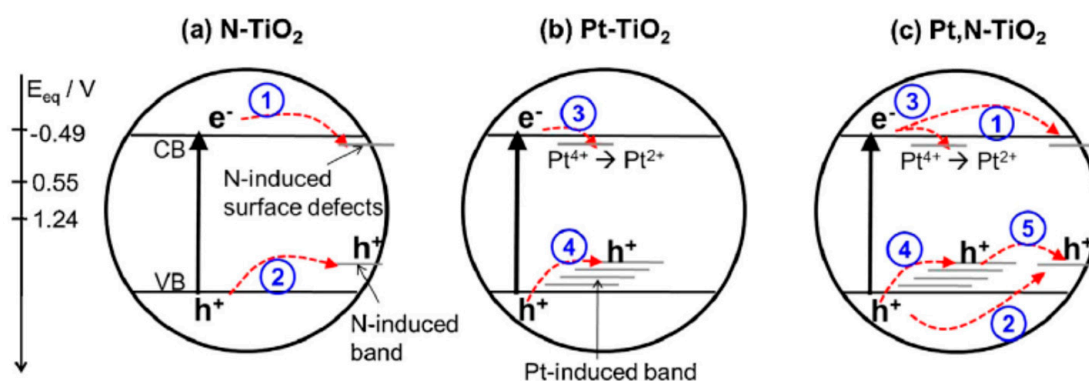


Figure 17. Schematic illustration for electron and hole trapping in (a) N-TiO₂, (b) Pt-TiO₂ and (c) Pt,N-TiO₂ under 355 nm irradiation. The numbers refer to charge transfer steps: (1) electron trapping on the defect site, (2) hole trapping on the N-induced states, (3) intervalent charge transfer or transition of Pt⁴⁺ to Pt²⁺, (4) localization of holes on the Pt-induced band and (5) hole-hopping. Reprinted from [74], Copyright 2020, with permission from Elsevier.

The superiority of Pt,N-TiO₂ photocatalyst for acetaldehyde oxidation observed by the researchers could be attributed to the presence of the new impurity doping levels created by the co-doped Pt and N species and/or the change in the charge transfer dynamics and kinetics [74].

Other researchers [73] observed photocatalytic activity of TiO₂ co-doped with nitrogen and different metals under visible light ($\lambda > 410$ nm) for acetaldehyde decomposition. They found that photocatalytic activity over TiO_{2-x}N_x was markedly enhanced by Cu or Pt loading, while Ni-, Zn- or La-loaded TiO_{2-x}N_x showed a similar photodegradation rate to the bare TiO_{2-x}N_x. Among them, the enhancement effect of Cu ion was found to be the highest. The optimum concentration of Cu was found to be 0.5 wt.% and nitrogen concentration around 0.25 at.%. Figure 18 shows the formation of CO₂ upon acetaldehyde oxidation under visible light with TiO₂ doped with nitrogen and co-doped with nitrogen and Cu [73].

Thermo-photocatalytic decomposition was observed for titania samples loaded with platinum nanoparticles [79,84]. The extremely high rate of formic acid oxidation over Pt-TiO_{2-x}N_x was found to be due to a combined effect of both photocatalysis and thermal catalysis at room temperature, facilitated by nanosized (1–2 nm) Pt [79]. The other researchers noted increased decomposition rate of acetaldehyde by decreasing distance between photocatalyst (Pt-TiO₂/SiO₂) and the source of light used in the process [84]. They observed that in the presence of platinum, byproducts and coke precursors were easily burned. For that reason, the combination of the catalytic properties of some metals with the photocatalytic activity of TiO₂ seems to be a very interesting and promising solution for the complete

decomposition of VOCs compounds. Fujishima et al. reported that during weak UV irradiation used for acetaldehyde decomposition, acetic acid was quantitatively formed as the main byproduct of the photocatalytic process, and its amount was increasing with the decrease of the number of absorbed photons [85]. The authors noted ca. 150% maximum quantum yield for acetaldehyde conversion to acetic acid, which was a result of a radical chain-type process with a chain length of approximately five [85]. Although conversion of acetaldehyde during photocatalytic reactions carried out on doped TiO₂ is possible to be higher than on the undoped titania, quantitative formation of byproducts decreases the mineralization degree. For instance, Mn-doped TiO₂ indicated activity under visible light and higher conversion of acetaldehyde under visible light irradiation than TiO₂. On the other hand, formation of CO₂ on the former photocatalyst was confirmed to be much lower than on the latter one [78]. Other researchers investigated the commercial TiO₂ KRONOClean[®]7000 for acetaldehyde decomposition under irradiation with light emitted by a fluorescent lamp, and they observed formaldehyde as the main byproduct of acetaldehyde conversion [12]. Some metal species doped to TiO₂ can act as a catalyst and thus support the complete oxidation of acetaldehyde. Efficient decomposition of acetaldehyde under visible light irradiation by TiO₂ co-doped with Cu and Co was reported [76]. The main products of acetaldehyde conversion were H₂O and CO₂ [76]. Doping some noble metals like Ag, Au, Pt or Pd to TiO₂ results in obtaining materials revealing enhanced photocatalytic activity under visible light. The observed enhancement is due to efficient transport of electrons generated over the doped nanoparticles by local surface plasmon resonance (LSPR), across the metal/semiconductor interface via the defect states of TiO₂ [75]. Another way of increasing activity of TiO₂ under visible light is preparation of composites of titania with another semiconductor, revealing lower energy of the band gap being able to absorb the photons induced by the visible light [80,81]. In such modified titania, photoinduced transport of electrons occurs between both semiconductors and improvement of the charge separation process takes place.

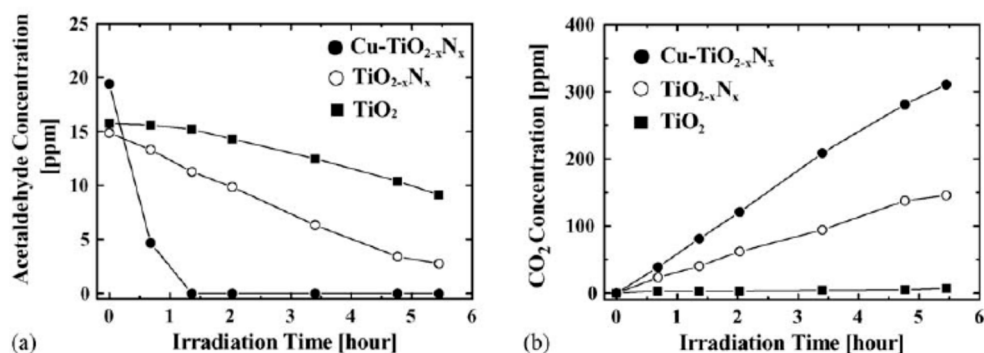


Figure 18. Concentrations of acetaldehyde (a) and CO₂ (b), as a function of visible light irradiation time on bare TiO₂, TiO_{2-x}N_x and Cu-loaded TiO_{2-x}N_x. Reprinted from [73], Copyright 2020, with permission from Elsevier.

6. Conclusions

TiO₂ appears to be an effective photocatalyst for decomposition of VOCs such as acetaldehyde. However, effective exploitation requires controlling different parameters, such as humidity of the ambient air, intensity of the light or concentrations of the contaminants. At the conditions of high relative humidity, such as 50%, the contact of acetaldehyde gas with the active sites of TiO₂ will be limited, and its conversion to CO₂ will not be high. For low-intensity UV light, conversion of acetaldehyde would proceed to high yield of acetic acid or to the formation of formaldehyde, without its complete mineralization. The presence of surface defects on the titania surface can enhance the process of the photocatalytic decomposition of acetaldehyde. However, oxygen vacancies formed in TiO₂ appeared to be detrimental to this process. Acetaldehyde molecules adsorb on the oxygen vacancy sites by the oxygen group. The oxygen vacancies after saturation with oxygen are not regenerated.

Adsorbed acetaldehyde molecules on the oxygen vacancy sites can reduce the adsorption of oxygen molecules and diminish the formation of superoxide radicals. In case of surface defects formed without oxygen vacancies, the oxygen molecules are adsorbed on the defect sites of TiO₂ and they can be utilized as superoxide radicals, which are very effective in the photocatalytic decomposition of gaseous acetaldehyde.

Doping of some metallic species to TiO₂ can increase the photocatalytic degradation and mineralization of acetaldehyde through either the induced catalytic or thermo-catalytic processes. However, such effect has been observed only after doping to TiO₂ metallic particles with a size of a few nm. Application of visible light for the photocatalytic decomposition of acetaldehyde appears to be less efficient than under UV, and the total mineralization degree of acetaldehyde is usually attained after a much longer time than that during exposure to UV or UV-Vis irradiations. Therefore, the future perspectives of TiO₂ application for VOCs decomposition can be realized by developing a smart-designed photoreactor equipped in UV lamps (LED type UV lamps are preferable, because of the low power consumption and narrow spectrum of emitted light). Moreover, a photocatalyst inside the reactor should be distributed in a way that facilitates a good contact of the treated gas with the photocatalytic surface. Additionally, drying of the inlet gas before its further treatment over the photocatalytic process is recommended to be carried out to increase the efficiency of the contaminants' degradation process. In case of TiO₂ doped with catalytically active metallic species, the space between lamps and the photoactive surface should be small enough to induce the thermo-photocatalytic process. Because longer contact time of reactant gas with the active surface of photocatalyst increases the efficiency of VOCs degradation, the flow rate of the treated gas should be fitted to maximize diffusion of contaminants to the photocatalyst surface.

Author Contributions: B.T.—wrote the manuscript, analyses and interpretation of the results; P.R.—performed experiments and figures, analyses of the results; A.M.-S.—overview of the literature, J.P.—supervision. All authors have read and agreed to the published version of the manuscript.

Funding: This research received no external funding.

Conflicts of Interest: The authors declare no conflict of interest.

References

1. Burge, P.S. Sick building syndrome. *Occup. Environ. Med.* **2004**, *61*, 185–190. [[CrossRef](#)] [[PubMed](#)]
2. Xiao, R.; Mo, J.; Zhang, Y.; Gao, D. An in-situ thermally regenerated air purifier for indoor formaldehyde removal. *Indoor Air* **2018**, *28*, 266–275. [[CrossRef](#)] [[PubMed](#)]
3. Ao, C.H.; Lee, S.C. Indoor air purification by photocatalyst TiO₂ immobilized on an activated carbon filter installed in an air cleaner. *Chem. Eng. Sci.* **2005**, *60*, 103–109. [[CrossRef](#)]
4. Yu, Q.L.; Ballari, M.M.; Brouwers, H.J.H. Indoor air purification using heterogeneous photocatalytic oxidation. Part II: Kinetic study. *Appl. Catal. B Environ.* **2010**, *99*, 58–65. [[CrossRef](#)]
5. Haghghatmamaghani, A.; Haghghat, F.; Lee, C.-S. Performance of various commercial TiO₂ in photocatalytic degradation of a mixture of indoor air pollutants: Effect of photocatalyst and operating parameters. *Sci. Technol. Built Environ.* **2019**, *25*, 600–614. [[CrossRef](#)]
6. Hamidi, F.; Aslani, F. TiO₂-based Photocatalytic Cementitious Composites: Materials, Properties, Influential Parameters, and Assessment Techniques. *Nanomaterials* **2019**, *9*, 1444. [[CrossRef](#)] [[PubMed](#)]
7. Tryba, B.; Homa, P.; Wróbel, R.J.; Morawski, A.W. Photocatalytic decomposition of benzo-[a]-pyrene on the surface of acrylic, latex and mineral paints. Influence of paint composition. *J. Photochem. Photobiol. Chem.* **2014**, *286*, 10–15. [[CrossRef](#)]
8. Chen, J.; Poon, C. Photocatalytic construction and building materials: From fundamentals to applications. *Built Environ.* **2009**, *44*, 1899–1906. [[CrossRef](#)]
9. Mills, A.; Hill, C.; Robertson, P.K.J. Overview of the current ISO tests for photocatalytic materials. *J. Photochem. Photobiol. Chem.* **2012**, *237*, 7–23. [[CrossRef](#)]
10. Fujishima, A.; Rao, T.N.; Tryk, D.A. Titanium dioxide photocatalysis. *J. Photochem. Photobiol. C Photochem. Rev.* **2000**, *1*, 1–21. [[CrossRef](#)]

11. Melchers, S.; Schneider, J.; Emeline, A.; Bahnemann, D. Effect of H₂O and O₂ on the Adsorption and Degradation of Acetaldehyde on Anatase Surfaces—An In Situ ATR-FTIR Study. *Catalysts* **2018**, *8*, 417. [[CrossRef](#)]
12. Salvadores, F.; Minen, R.I.; Carballada, J.; Alfano, O.M.; Ballari, M.M. Kinetic Study of Acetaldehyde Degradation Applying Visible Light Photocatalysis. *Chem. Eng. Technol.* **2016**, *39*, 166–174. [[CrossRef](#)]
13. Tryba, B.; Rychtowski, P.; Srenscek-Nazzal, J.; Przepiorski, J. The influence of TiO₂ structure on the complete decomposition of acetaldehyde gas. *Mater. Res. Bull.* **2020**, *126*, 110816. [[CrossRef](#)]
14. Plata, J.J.; Collico, V.; Márquez, A.M.; Sanz, J.F. Understanding Acetaldehyde Thermal Chemistry on the TiO₂ (110) Rutile Surface: From Adsorption to Reactivity. *J. Phys. Chem. C* **2011**, *115*, 2819–2825. [[CrossRef](#)]
15. Zeng, Q.; Wang, X.; Xie, X.; Mahmood, A.; Lu, G.; Wang, Y.; Sun, J. Band bending of TiO₂ induced by O-xylene and acetaldehyde adsorption and its effect on the generation of active radicals. *J. Colloid Interface Sci.* **2020**, *572*, 374–383. [[CrossRef](#)]
16. Liu, Z.; Zhang, X.; Nishimoto, S.; Murakami, T.; Fujishima, A. Efficient Photocatalytic Degradation of Gaseous Acetaldehyde by Highly Ordered TiO₂ Nanotube Arrays. *Environ. Sci. Technol.* **2008**, *42*, 8547–8551. [[CrossRef](#)]
17. Stefanov, B.I.; Niklasson, G.A.; Granqvist, C.G.; Österlund, L. Gas-phase photocatalytic activity of sputter-deposited anatase TiO₂ films: Effect of (0 0 1) preferential orientation, surface temperature and humidity. *J. Catal.* **2016**, *335*, 187–196. [[CrossRef](#)]
18. Young, Z.D.; Hanspal, S.; Davis, R.J. Aldol Condensation of Acetaldehyde over Titania, Hydroxyapatite, and Magnesia. *ACS Catal.* **2016**, *6*, 3193–3202. [[CrossRef](#)]
19. Hauchecorne, B.; Terrens, D.; Verbruggen, S.; Martens, J.A.; Van Langenhove, H.; Demeestere, K.; Lenaerts, S. Elucidating the photocatalytic degradation pathway of acetaldehyde: An FTIR in situ study under atmospheric conditions. *Appl. Catal. B Environ.* **2011**, *106*, 630–638. [[CrossRef](#)]
20. Batault, F.; Thevenet, F.; Hequet, V.; Rillard, C.; Le Coq, L.; Locoge, N. Acetaldehyde and acetic acid adsorption on TiO₂ under dry and humid conditions. *Chem. Eng. J.* **2015**, *264*, 197–210. [[CrossRef](#)]
21. Tryba, B.; Tygielska, M.; Orlikowski, J.; Przepiorski, J. Influence of TiO₂ hydrophilicity on the photocatalytic decomposition of gaseous acetaldehyde in a circulated flow reactor. *React. Kinet. Mech. Catal.* **2016**, *119*, 349–365. [[CrossRef](#)]
22. Jiang, Y.; Amal, R. Selective synthesis of TiO₂-based nanoparticles with highly active surface sites for gas-phase photocatalytic oxidation. *Appl. Catal. B Environ.* **2013**, *138–139*, 260–267. [[CrossRef](#)]
23. Banerjee, S.; Dionysiou, D.D.; Pillai, S.C. Self-cleaning applications of TiO₂ by photo-induced hydrophilicity and photocatalysis. *Appl. Catal. B Environ.* **2015**, *176–177*, 396–428. [[CrossRef](#)]
24. Xu, X.; Zhu, J. Hydrothermal Synthesis of TiO₂ Nanoparticles for Photocatalytic Degradation of Ethane: Effect of Synthesis Conditions. *Recent Pat. Chem. Eng.* **2012**, *5*, 134–142. [[CrossRef](#)]
25. Tryba, B.; Tygielska, M.; Colbeau-Justin, C.; Kusiak-Nejman, E.; Kapica-Kozar, J.; Wróbel, R.; Żońnierkiewicz, G.; Guskos, N. Influence of pH of sol-gel solution on phase composition and photocatalytic activity of TiO₂ under UV and visible light. *Mater. Res. Bull.* **2016**, *84*, 152–161. [[CrossRef](#)]
26. Byun, D.; Jin, Y.; Kim, B.; Kee Lee, J.; Park, D. Photocatalytic TiO₂ deposition by chemical vapor deposition. *J. Hazard. Mater.* **2000**, *73*, 199–206. [[CrossRef](#)]
27. Aguilar, T.; Carrillo-Berdugo, I.; Gómez-Villarejo, R.; Gallardo, J.; Martínez-Merino, P.; Piñero, J.; Alcántara, R.; Fernández-Lorenzo, C.; Navas, J. A Solvothermal Synthesis of TiO₂ Nanoparticles in a Non-Polar Medium to Prepare Highly Stable Nanofluids with Improved Thermal Properties. *Nanomaterials* **2018**, *8*, 816. [[CrossRef](#)]
28. Chen, X.; Xu, Z.; Yang, F.; Zhao, H. Flame spray pyrolysis synthesized CuO-TiO₂ nanoparticles for catalytic combustion of lean CO. *Proc. Combust. Inst.* **2019**, *37*, 5499–5506. [[CrossRef](#)]
29. Sahrin, N.T.; Nawaz, R.; Fai Kait, C.; Lee, S.L.; Wirzal, M.D.H. Visible Light Photodegradation of Formaldehyde over TiO₂ Nanotubes Synthesized via Electrochemical Anodization of Titanium Foil. *Nanomaterials* **2020**, *10*, 128. [[CrossRef](#)]
30. Hosseini Zori, M. Synthesis of TiO₂ Nanoparticles by Microemulsion/Heat Treated Method and Photodegradation of Methylene Blue. *J. Inorg. Organomet. Polym. Mater.* **2011**, *21*, 81–90. [[CrossRef](#)]
31. Nateq, M.H.; Ceccato, R. Sol-Gel Synthesis of TiO₂ Nanocrystalline Particles with Enhanced Surface Area through the Reverse Micelle Approach. *Adv. Mater. Sci. Eng.* **2019**, *2019*, 1–14. [[CrossRef](#)]
32. Wang, J.; Zhu, W.; Zhang, Y.; Liu, S. An Efficient Two-Step Technique for Nitrogen-Doped Titanium Dioxide Synthesizing: Visible-Light-Induced Photodecomposition of Methylene Blue. *J. Phys. Chem. C* **2007**, *111*, 1010–1014. [[CrossRef](#)]

33. Pitchaimuthu, S.; Honda, K.; Suzuki, S.; Naito, A.; Suzuki, N.; Katsumata, K.; Nakata, K.; Ishida, N.; Kitamura, N.; Idemoto, Y.; et al. Solution Plasma Process-Derived Defect-Induced Heterophase Anatase/Brookite TiO₂ Nanocrystals for Enhanced Gaseous Photocatalytic Performance. *ACS Omega* **2018**, *3*, 898–905. [[CrossRef](#)] [[PubMed](#)]
34. Carrera, R.; Vázquez, A.L.; Castillo, S.; Arce Estrada, E.M. Photocatalytic Degradation of Acetaldehyde by Sol-Gel TiO₂ Nanoparticles: Effect of the Physicochemical Properties on the Photocatalytic Activity. *Mater. Sci. Forum* **2011**, *691*, 92–98. [[CrossRef](#)]
35. Tryba, B.; Jafari, S.; Sillanpää, M.; Nitta, A.; Ohtani, B.; Morawski, A.W. Influence of TiO₂ structure on its photocatalytic activity towards acetaldehyde decomposition. *Appl. Surf. Sci.* **2019**, *470*, 376–385. [[CrossRef](#)]
36. Di Paola, A.; Bellardita, M.; Palmisano, L. Brookite, the Least Known TiO₂ Photocatalyst. *Catalysts* **2013**, *3*, 36–73. [[CrossRef](#)]
37. Hu, Y.; Xie, X.; Wang, X.; Wang, Y.; Zeng, Y.; Pui, D.Y.H.; Sun, J. Visible-Light Upconversion Carbon Quantum Dots Decorated TiO₂ for the Photodegradation of Flowing Gaseous Acetaldehyde. *Appl. Surf. Sci.* **2018**, *440*, 266–274. [[CrossRef](#)]
38. Sopyan, I. Kinetic analysis on photocatalytic degradation of gaseous acetaldehyde, ammonia and hydrogen sulfide on nanosized porous TiO₂ films. *Sci. Technol. Adv. Mater.* **2007**, *8*, 33–39. [[CrossRef](#)]
39. Fan, X.; Yu, T.; Zhang, L.; Chen, X.; Zou, Z. Photocatalytic Degradation of Acetaldehyde on Mesoporous TiO₂: Effects of Surface Area and Crystallinity on the Photocatalytic Activity. *Chin. J. Chem. Phys.* **2007**, *20*, 733–738. [[CrossRef](#)]
40. Tseng, T.K.; Lin, Y.S.; Chen, Y.J.; Chu, H. A Review of Photocatalysts Prepared by Sol-Gel Method for VOCs Removal. *Int. J. Mol. Sci.* **2010**, *11*, 2336–2361. [[CrossRef](#)]
41. Liang, Y.; Sun, S.; Deng, T.; Ding, H.; Chen, W.; Chen, Y. The Preparation of TiO₂ Film by the Sol-Gel Method and Evaluation of Its Self-Cleaning Property. *Materials* **2018**, *11*, 450. [[CrossRef](#)] [[PubMed](#)]
42. Niemelä, J.-P.; Marin, G.; Karppinen, M. Titanium dioxide thin films by atomic layer deposition: A review. *Semicond. Sci. Technol.* **2017**, *32*, 093005. [[CrossRef](#)]
43. Verbruggen, S.W.; Deng, S.; Kurttepel, M.; Cott, D.J.; Vereecken, P.M.; Bals, S.; Martens, J.A.; Detavernier, C.; Lenaerts, S. Photocatalytic acetaldehyde oxidation in air using spacious TiO₂ films prepared by atomic layer deposition on supported carbonaceous sacrificial templates. *Appl. Catal. B Environ.* **2014**, *160–161*, 204–210. [[CrossRef](#)]
44. Yin, Q.; Xiang, J.; Wang, X.; Guo, X.; Zhang, T. Preparation of highly crystalline mesoporous TiO₂ by sol-gel method combined with two-step calcining process. *J. Exp. Nanosci.* **2016**, *11*, 1127–1137. [[CrossRef](#)]
45. Xu, H.; Vanamu, G.; Nie, Z.; Konishi, H.; Yeredla, R.; Phillips, J.; Wang, Y. Photocatalytic Oxidation of a Volatile Organic Component of Acetaldehyde Using Titanium Oxide Nanotubes. *J. Nanomater.* **2006**, *2006*, 1–8. [[CrossRef](#)]
46. Hernández-Alonso, M.D.; García-Rodríguez, S.; Suárez, S.; Portela, R.; Sánchez, B.; Coronado, J.M. Highly selective one-dimensional TiO₂-based nanostructures for air treatment applications. *Appl. Catal. B Environ.* **2011**, *110*, 251–259. [[CrossRef](#)]
47. Yu, J.; Wang, D.; Huang, Y.; Fan, X.; Tang, X.; Gao, C.; Li, J.; Zou, D.; Wu, K. A cylindrical core-shell-like TiO₂ nanotube array anode for flexible fiber-type dye-sensitized solar cells. *Nanoscale Res. Lett.* **2011**, *6*, 94. [[CrossRef](#)]
48. Lin, L.-Y.; Yeh, M.-H.; Chen, W.-C.; Ramamurthy, V.; Ho, K.-C. Controlling Available Active Sites of Pt-Loaded TiO₂ Nanotube-Imprinted Ti Plates for Efficient Dye-Sensitized Solar Cells. *ACS Appl. Mater. Interfaces* **2015**, *7*, 3910–3919. [[CrossRef](#)]
49. Nischk, M.; Mazierski, P.; Gazda, M.; Zaleska, A. Ordered TiO₂ nanotubes: The effect of preparation parameters on the photocatalytic activity in air purification process. *Appl. Catal. B Environ.* **2014**, *144*, 674–685. [[CrossRef](#)]
50. Pichat, P. Are TiO₂ Nanotubes Worth Using in Photocatalytic Purification of Air and Water? *Molecules* **2014**, *19*, 15075–15087. [[CrossRef](#)]
51. Ahn, K.; Kim, M.-S.; Kim, S.-H.; Hyun Kim, J.; Jeong, S.-Y.; Kim, J.-P.; Sung Jin, J.; Cho, C.-R. Optical properties of hierarchical-nanostructured TiO₂ and its time-dependent photo-degradation of gaseous acetaldehyde. *Appl. Phys. Lett.* **2013**, *103*, 261903. [[CrossRef](#)]
52. Pan, C.; Dong, L. Fabrication of Gold-Doped Titanium Dioxide (TiO₂:Au) Nanofibers Photocatalyst by Vacuum Ion Sputter Coating. *J. Macromol. Sci. Part B* **2009**, *48*, 919–926. [[CrossRef](#)]
53. Hai-Qin, C.; Li-Qiang, J.; Ming-Zheng, X.; Zhi-Jun, L. Hydrogenated Rutile TiO₂ Nanorods and Their Photocatalytic Activity. *Acta Phys. Chim. Sin.* **2014**, *30*, 1903–1908. [[CrossRef](#)]

54. Finkelstein-Shapiro, D.; Buchbinder, A.M.; Vijayan, B.; Bhattacharyya, K.; Weitz, E.; Geiger, F.M.; Gray, K.A. Identification of Binding Sites for Acetaldehyde Adsorption on Titania Nanorod Surfaces Using CIMS. *Langmuir* **2011**, *27*, 14842–14848. [[CrossRef](#)] [[PubMed](#)]
55. Ohno, T.; Higo, T.; Saito, H.; Yuajn, S.; Jin, Z.; Yang, Y.; Tsubota, T. Dependence of photocatalytic activity on aspect ratio of a brookite TiO₂ nanorod and drastic improvement in visible light responsibility of a brookite TiO₂ nanorod by site-selective modification of Fe³⁺ on exposed faces. *J. Mol. Catal. Chem.* **2015**, *396*, 261–267. [[CrossRef](#)]
56. Bae, E.; Murakami, N.; Ohno, T. Exposed crystal surface-controlled TiO₂ nanorods having rutile phase from TiCl₃ under hydrothermal conditions. *J. Mol. Catal. Chem.* **2009**, *300*, 72–79. [[CrossRef](#)]
57. Ohno, T.; Sarukawa, K.; Matsumura, M. Crystal faces of rutile and anatase TiO₂ particles and their roles in photocatalytic reactions. *New J. Chem.* **2002**, *26*, 1167–1170. [[CrossRef](#)]
58. Ji, Y.; Zheng, Y.; Ma, X.; Cui, X.; Wang, B. Role of reduced defects for coupling reactions of acetaldehyde on anatase TiO₂(001)-(1 × 4) surface. *Chin. J. Chem. Phys.* **2019**, *32*, 417–422. [[CrossRef](#)]
59. Mahmood, A.; Shi, G.; Xie, X.; Sun, J. Assessing the adsorption and photocatalytic activity of TiO₂ nanoparticles for the gas phase acetaldehyde: A computational and experimental study. *J. Alloys Compd.* **2020**, *819*, 153055. [[CrossRef](#)]
60. Rekoske, J.E.; Barteau, M.A. Kinetics, Selectivity, and Deactivation in the Aldol Condensation of Acetaldehyde on Anatase Titanium Dioxide. *Ind. Eng. Chem. Res.* **2011**, *50*, 41–51. [[CrossRef](#)]
61. Tryba, B.; Wozniak, M.; Zolnierkiewicz, G.; Guskos, N.; Morawski, A.; Colbeau-Justin, C.; Wrobel, R.; Nitta, A.; Ohtani, B. Influence of an Electronic Structure of N-TiO₂ on Its Photocatalytic Activity towards Decomposition of Acetaldehyde under UV and Fluorescent Lamps Irradiation. *Catalysts* **2018**, *8*, 85. [[CrossRef](#)]
62. Topalian, Z.; Stefanov, B.I.; Granqvist, C.G.; Österlund, L. Adsorption and photo-oxidation of acetaldehyde on TiO₂ and sulfate-modified TiO₂: Studies by in situ FTIR spectroscopy and micro-kinetic modeling. *J. Catal.* **2013**, *307*, 265–274. [[CrossRef](#)]
63. Buchalska, M.; Kobielski, M.; Matuszek, A.; Pacia, M.; Wojtyła, S.; Macyk, W. On Oxygen Activation at Rutile- and Anatase-TiO₂. *ACS Catal.* **2015**, *5*, 7424–7431. [[CrossRef](#)]
64. Zehr, R.T.; Henderson, M.A. Acetaldehyde photochemistry on TiO₂(110). *Surf. Sci.* **2008**, *602*, 2238–2249. [[CrossRef](#)]
65. Asahi, R. Visible-Light Photocatalysis in Nitrogen-Doped Titanium Oxides. *Science* **2001**, *293*, 269–271. [[CrossRef](#)]
66. Meroni, D.; Ardizzone, S.; Cappelletti, G.; Oliva, C.; Ceotto, M.; Poelman, D.; Poelman, H. Photocatalytic removal of ethanol and acetaldehyde by N-promoted TiO₂ films: The role of the different nitrogen sources. *Catal. Today* **2011**, *161*, 169–174. [[CrossRef](#)]
67. Lin, Y.-H.; Weng, C.-H.; Tzeng, J.-H.; Lin, Y.-T. Adsorption and Photocatalytic Kinetics of Visible-Light Response N-Doped TiO₂ Nanocatalyst for Indoor Acetaldehyde Removal under Dark and Light Conditions. *Int. J. Photoenergy* **2016**, *2016*, 1–9. [[CrossRef](#)]
68. Nishijima, K.; Naitoh, H.; Tsubota, T.; Ohno, T. Visible-Light-Induced Hydrophilic Conversion of an S-Doped TiO₂ Thin Film and Its Photocatalytic Activity for Decomposition of Acetaldehyde in Gas Phase. *J. Ceram. Soc. Jpn.* **2007**, *115*, 310–314. [[CrossRef](#)]
69. Khalilzadeh, A.; Fatemi, S. Modification of nano-TiO₂ by doping with nitrogen and fluorine and study acetaldehyde removal under visible light irradiation. *Clean Technol. Environ. Policy* **2014**, *16*, 629–636. [[CrossRef](#)]
70. Ballari, M.M.; Carballada, J.; Minen, R.I.; Salvadores, F.; Brouwers, H.J.H.; Alfano, O.M.; Cassano, A.E. Visible light TiO₂ photocatalysts assessment for air decontamination. *Process Saf. Environ. Prot.* **2016**, *101*, 124–133. [[CrossRef](#)]
71. Boningari, T.; Inturi, S.N.R.; Suidan, M.; Smirniotis, P.G. Novel one-step synthesis of sulfur doped-TiO₂ by flame spray pyrolysis for visible light photocatalytic degradation of acetaldehyde. *Chem. Eng. J.* **2018**, *339*, 249–258. [[CrossRef](#)]
72. Hamal, D.B.; Klabunde, K.J. Synthesis, characterization, and visible light activity of new nanoparticle photocatalysts based on silver, carbon, and sulfur-doped TiO₂. *J. Colloid Interface Sci.* **2007**, *311*, 514–522. [[CrossRef](#)] [[PubMed](#)]
73. Morikawa, T.; Irokawa, Y.; Ohwaki, T. Enhanced photocatalytic activity of TiO₂-_xN_x loaded with copper ions under visible light irradiation. *Appl. Catal. Gen.* **2006**, *314*, 123–127. [[CrossRef](#)]
74. Kim, W.; Tachikawa, T.; Kim, H.; Lakshminarasimhan, N.; Murugan, P.; Park, H.; Majima, T.; Choi, W. Visible light photocatalytic activities of nitrogen and platinum-doped TiO₂: Synergistic effects of co-dopants. *Appl. Catal. B Environ.* **2014**, *147*, 642–650. [[CrossRef](#)]

75. Song, H.; Yu, Y.-T.; Norby, P. Efficient Complete Oxidation of Acetaldehyde into CO₂ Over Au/TiO₂ Core–Shell Nano Catalyst Under UV and Visible Light Irradiation. *J. Nanosci. Nanotechnol.* **2009**, *9*, 5891–5897. [[CrossRef](#)]
76. Mohamed, R.M.; Bahnemann, D.W.; Basaleh, A.S.; Qadah, R.H. Photo-catalytic destruction of acetaldehyde using cobalt, copper co-doped titania dioxide nanoparticles beneath Visible light. *Appl. Nanosci.* **2020**, *10*, 931–939. [[CrossRef](#)]
77. Saqlain, S.; Cha, B.J.; Kim, S.Y.; Ahn, T.K.; Park, C.; Oh, J.-M.; Jeong, E.C.; Seo, H.O.; Kim, Y.D. Visible light-responsive Fe-loaded TiO₂ photocatalysts for total oxidation of acetaldehyde: Fundamental studies towards large-scale production and applications. *Appl. Surf. Sci.* **2020**, *505*, 144160. [[CrossRef](#)]
78. Papadimitriou, V.C.; Stefanopoulos, V.G.; Romanias, M.N.; Papagiannakopoulos, P.; Sambani, K.; Tudose, V.; Kiriakidis, G. Determination of photo-catalytic activity of un-doped and Mn-doped TiO₂ anatase powders on acetaldehyde under UV and visible light. *Thin Solid Films* **2011**, *520*, 1195–1201. [[CrossRef](#)]
79. Morikawa, T.; Ohwaki, T.; Suzuki, K.; Moribe, S.; Tero-Kubota, S. Visible-light-induced photocatalytic oxidation of carboxylic acids and aldehydes over N-doped TiO₂ loaded with Fe, Cu or Pt. *Appl. Catal. B Environ.* **2008**, *83*, 56–62. [[CrossRef](#)]
80. Muñoz-Batista, M.J.; de los Milagros Ballari, M.; Kubacka, A.; Cassano, A.E.; Alfano, O.M.; Fernández-García, M. Acetaldehyde degradation under UV and visible irradiation using CeO₂–TiO₂ composite systems: Evaluation of the photocatalytic efficiencies. *Chem. Eng. J.* **2014**, *255*, 297–306. [[CrossRef](#)]
81. Yamaguchi, Y.; Liu, B.; Terashima, C.; Katsumata, K.; Suzuki, N.; Fujishima, A.; Sakai, H.; Nakata, K. Fabrication of Efficient Visible-light-responsive TiO₂–WO₃ Hollow Particle Photocatalyst by Electrospray Method. *Chem. Lett.* **2017**, *46*, 122–124. [[CrossRef](#)]
82. Di Valentin, C.; Pacchioni, G.; Selloni, A.; Livraghi, S.; Giamello, E. Characterization of Paramagnetic Species in N-Doped TiO₂ Powders by EPR Spectroscopy and DFT Calculations. *J. Phys. Chem. B* **2005**, *109*, 11414–11419. [[CrossRef](#)] [[PubMed](#)]
83. Sakatani, Y.; Nunoshige, J.; Ando, H.; Okusako, K.; Koike, H.; Takata, T.; Kondo, J.N.; Hara, M.; Domen, K. Photocatalytic Decomposition of Acetaldehyde under Visible Light Irradiation over La³⁺ and N Co-doped TiO₂. *Chem. Lett.* **2003**, *32*, 1156–1157. [[CrossRef](#)]
84. Nakano, K.; Obuchi, E.; Nanri, M. Thermo-Photocatalytic Decomposition of Acetaldehyde Over Pt-TiO₂/SiO₂. *Chem. Eng. Res. Des.* **2004**, *82*, 297–301. [[CrossRef](#)]
85. Ohko, Y.; Tryk, D.A.; Hashimoto, K.; Fujishima, A. Autoxidation of Acetaldehyde Initiated by TiO₂ Photocatalysis under Weak UV Illumination. *J. Phys. Chem. B* **1998**, *102*, 2699–2704. [[CrossRef](#)]

Publisher's Note: MDPI stays neutral with regard to jurisdictional claims in published maps and institutional affiliations.



© 2020 by the authors. Licensee MDPI, Basel, Switzerland. This article is an open access article distributed under the terms and conditions of the Creative Commons Attribution (CC BY) license (<http://creativecommons.org/licenses/by/4.0/>).